Chapter 2
Recent Advances in Photocatalytic Degradation of Dyes Using Heterogeneous Catalysts

Bubul Das, Hirendra Nath Dhara, Anjali Dahiya, and Bhisma K. Patel

Abstract Synthetic dyes are playing a vital role in day-to-day life as different products ranging from textiles to leather to furniture contain dye for colouring purposes. It is reported that 12% of these dyes are wasted during processing. However, these industrial non-biodegradable dyes often enter water bodies such as groundwater, river, and lake and pollute them. Removal of these hazardous pollutants or dyes from wastewater has gained attention due to environmental concerns. Various techniques have been developed for the removal of these carcinogenic dyes from the natural environment. Degradation of dyes and eventually their removal from the mainstream and aquatic media using UV or visible light in the presence of photocatalyst (PC) are some reasonable technologies. Photocatalytic degradation (PD) could convert bio non-degradable dye complex molecules into smaller, non-carcinogenic, low molecular species. The process of PD is based on the generation of highly reactive, hydroxyl and superoxide anion radicals, which target the dye molecules and convert them into H_2O and CO_2. The chapter focuses on the principle and mechanism of dye degradation using heterogeneous photocatalyst. A brief discussion of the various important heterogeneous photocatalyst in the degradation of dye will be discussed in the latter part of the chapter.

Keywords Dyes · Degradation · Heterogeneous photocatalyst · Radicals · Advanced oxidation processes (AOPs)

2.1 Introduction

The development of science and technology leads us towards the new chemicals which are raw materials in various industrial processes. Organic dyes turned out to be one such chemical that is useful in different industrial activities for colouring various products. Though the textile dyeing industry has progressed a lot, initially

B. Das · H. N. Dhara · A. Dahiya · B. K. Patel (✉)
Department of Chemistry, Indian Institute of Technology Guwahati, Guwahati, Assam 781039, India
e-mail: patel@iitg.ac.in

S. Dave and J. Das (eds.), *Trends and Contemporary Technologies for Photocatalytic Degradation of Dyes*, Environmental Science and Engineering,
https://doi.org/10.1007/978-3-031-08991-6_2

nature was the sole source of dyes (Ferreira et al. 2004). Natural dyes can be obtained from animals, plants, minerals. Natural dyes are less harmful compared to synthetic dyes and they generate biodegradable wastewater (Silva et al. 2020). Synthetic dyes are organic compounds that are hydro or oil-soluble (Vázquez et al. 2020). The chemical structure of dyes is diverse, which include azo, nitro, phthalocyanine, and diarylmethane dyes having different chemical and physical properties (Belpaire et al. 2015). They are unsaturated complex organic compounds and can absorb light and emit colour in the visible region (Rehman et al. 2020). At present more than 100,000 dyes are commercially available and are being used increasingly in textile, rubber, plastic, cosmetics, food industries, and pharmaceuticals. Industrial effluents pollution is mainly caused by the increasing use of these dyes in the dyeing process. Biological treatment processes can be used for the treatment of wastewater containing high concentrations of biodegradable pollutants. However, low biodegradable toxic pollutants released from the textile (Touati et al. 2016), pharmaceutical (Olama et al. 2018), and agricultural industries (Kushniarou et al. 2019) are found in groundwater, surface water, and in municipal sewage treatment plant. Due to the incomplete removal of these dyes from wastewater, persistent organic pollutants with complex compositions remain in waterbodies. The wastewater from the dye industry is distinguished from others by high chemical oxygen demand (COD), total solids (TS), pH, biological oxygen demand (BOD), water usage, and colour. A ratio of 0.25 between biological oxygen demand to chemical oxygen demand indicates that industrial wastewater contains vast non-biodegradable organic materials. Water pollution related to dye contamination is life-threatening and harmful to the surrounding environments. Dye accumulation significantly affects aquatic life by increasing BOD and COD. This also inhibits plant growth as it impairs photosynthesis and human being by entering the food chain (Rehman et al. 2019; Tayade et al. 2009). The bulky size and complex structure of these dye molecules make them non-biodegradable, mutagenic as well as carcinogenic (Saeed et al. 2015). The annual worldwide production of synthetic dyes is around 7×10^5 tons for the textile industry. Out of these, 10–15% of these dyes do not bind to the fabrics during the dyeing process and enter directly into wastewater (Chandanshive et al. 2018). These unbound portions of dyes are found in very high concentrations in the textile effluents and directly enter into the wastewater (Drumond et al. 2013). The release of these dye-contaminated effluents into waterbodies is undesirable due to the non-biodegradable nature of dyes and their breakdown into hazardous intermediate products. The high tinctorial value of less than a ppm of dye in water could produce highly coloured elements and lead to aesthetic issues. In addition, the uncontrolled contaminations also retard the penetration of light through water, thus significantly affects the photosynthesis function of aquatic plants (Sahoo et al. 2012; Akpan and Hameed 2009).

Dye pollutants threaten the equilibrium of the food chain as it hampers the growth of photoautotrophic organisms by increasing the BOD of the waterbodies. These recalcitrant dyes are claimed to promote toxicity, carcinogenicity, mutagenicity, genotoxicity, teratogenicity, and their long-term exposure might affect the structure of ecosystems (Holkar et al. 2016). For example, crystal violet, acid violet, and malachite green which belong totriphenylmethane class of dyes are found to be

phototoxic to plants, cytotoxic to mammalian cells and even induce tumour growth in some aquatic species. Oral ingestion, inhalation, or workers in the field of dye manufacturing and processing may have skin and eyes abnormality, insomnia, immune suppression, asthma, allergic conjunctivitis, contact dermatitis or nasal problems on prolonged exposure to these dyes (Jadhav et al. 2012). The potential toxicity of these dyes and their high concentrations in the industrial effluents need to be carefully addressed.

Elimination of these dyes from contaminated water is a key environmental concern. Access to clean and toxic-free, carcinogenic agents free and harmful microbes free water is the need of the hour and draw special research attention to ensure smooth survival of human being in the near future. The conventional wastewater treatment is unsuccessful in the degradation and subsequent removal of these dyes from water bodies. The complex chemical structure and strong photocatalytic stability of dyes make them resistant to temperature, water, soap, and microbial attack. As a large variety of dyes are produced worldwide, various physical, chemical, and biological methods are available for their degradation and removal. These include adsorption (Wang et al. 2020), biosorption (Sharma et al. 2018), ozonation (Sripiboon et al. 2018), coagulation/flocculation (Zahrim and Hilal 2013), reverse osmosis (Abid et al. 2012), ultrafiltration (Ben et al. 2019), nanofiltration (Kong et al. 2019), electrochemical degradation (Moura et al. 2016), biodegradation (Ajaz et al. 2019), hybrid biological treatment (Zhang et al. 2017), advanced oxidation processes (AOPs) (Rauf and Ashraf 2009), etc. All these processes have their advantages and disadvantages over other methods. The high chemical stability of these dyes makes the conventional treatment method ineffective. Practical employment of these methods has limitations considering their efficiency, practicability, sludge production, reliability, feasibility, pre-treatment requirements, operation difficulty, and by-products generation (Crini and Lichtfouse 2019). A balanced approach is therefore necessary for choosing an appropriate method for dyes degradation. Out of these techniques mentioned above, the AOPs found to be promising green methods and have been reported to be effective for removing soluble organic pollutants. The AOPs can provide an almost total degradation of contaminant dyes and it is recognized as one of the most accepted techniques for controlling environmental pollution.

Heterogeneous photocatalysis is considered as one of the most recognized AOPs. Photocatalysis is a green approach over other traditional dye removal techniques for its simple, cost-effectiveness, high performance at even ambient temperature and complete mineralization of pollutants to ppm or ppb level (Zheng et al. 2019). Since the discovery of photoelectrochemical water splitting reaction by Fujishima and Honda (1972), photocatalysis has developed rapidly (Fujishima and Honda 1972). Photocatalysis is defined as the process in which the rate of the chemical reaction increases in the presence of some photocatalyst via the generation of electron–hole pairs when irradiated in the presence of UV/visible light. Photocatalysis is advantageous for low biodegradable, highly complex, and high concentrations of pollutants in wastewater. Photodegradation (PD) harnesses solar or UV light for the breakdown of large complex molecules into smaller, non-toxic, and lower molecular weight species. Oxidation/reduction of organic pollutants is induced by light via some simple redox

reactions. The process is triggered by the initial absorption of a photon by photocatalysts in the UV, visible or IR spectral range. PD has been considered as an energy-saving technology as it directly converts light energy into chemical energy. UV photolysis, oxidants such as hydroxyl radicals, H_2O_2, ozone-assisted photooxidation, and UV photocatalytic oxidation are some of the adopted technologies for PD (Ray 2000). Being green in nature PD supersedes conventional methods in the field of environmental purification. Some unique advantages of PD are listed in Fig. 2.1.

PD is carried out in the presence of heterogeneous catalysts. These catalysts should be stable, non-toxic, recyclable, highly photoactive, and readily available. Appropriate bandgaps in semiconductors make them good photocatalysts as they can utilize the energy of the photon (Serpone and Emeline 2002). Different metal oxides are used as heterogeneous photocatalysts for the decolouration of dyes. Catalysts TiO_2 and ZnO are frequently used for photo degradation. The physical state of the metal oxides is different from the reactant phase, for which it is termed as heterogeneous photocatalysis. Limited thermal stability, separation problems after

Fig. 2.1 Key advantages and efficiency of PD technologies for dye removal

the reaction are some obvious challenges associated with homogenous photocatalysis (Haibach et al. 2012). Therefore, most of the researchers focus on heterogeneous PC, which is going to be addressed in this chapter.

2.2 Classification of Dyes

Dye is a substance with the property of absorbing part of visible light and shows complementary colour. They are complex unsaturated aromatic compounds and characterized by intense colour, high solubility, and stability. As the annual global production of dyes is increasing, their classification is important to have a comprehensive study. Classification of dyes is a very difficult process because of their diverse chemical structure. At present, around 10,000 structurally different dyes are used annually (Chequer et al. 2013). Large structural variations amongst dyes challenge their classification from one parameter's view. They can be classified into different groups depending on their source, chemical structure, solubility, and fibre type for which they are most compatible. The more or less colouration of certain dyes is linked with the chemical composition. The textile industry is highly dominated by azo dyes. Azo dyes are characterized by a double bond between two nitrogen atoms [–N=N–]. Furthermore, the presence of auxiliary functional groups such as amino, hydroxyl, sulfoxyl, and carboxyl make them amphoteric (Benkhaya et al. 2020). Dyes can be further sub-divided as acidic, basic (cationic), direct (substantive), reactive, disperse (non-ionic), sulfur, and vat dyes. Various types of dyes are discussed in Table 2.1. Dyes mainly consist of three important components viz. chromophores, auxochromes, and matrixes. The chromophores are some functional groups that help the dye in the absorption of light in the form of electromagnetic waves. The functional groups may be azo (–N=N–), nitro ($–NO_2$), nitroso (–N=O), carbonyl (–C=O), thiocarbonyl (–C=S) as well as alkenes (–C=C–). On the other hand, auxochromes are the colour-enhancing groups and help in the modification of the colour of the dyes. When present in the dye they increase the fibre affinity for colour and decrease the water solubility either by electron-withdrawing or donating nature. They may be acidic (–COOH, $–SO_3H$, –OH) or basic ($–NH_2$, –NHR, $–NR_2$). The rest of the atoms of the molecule is called matrix. In general, dyes are a complex combination of chromophoric, auxochromic, and conjugated aromatic structures (benzenes, anthracenes, perylenes, etc.). Conjugation of the dyes increases with an increase in the number of aromatic rings. This conjugation leads to a redshift in absorption. Similarly, an electron donor auxochromic group when situated along with a conjugated system joins in the conjugation and the molecule absorbs in the longer wavelength and gives darkintense colour (Benkhaya et al. 2020).

Dyes are also classified based on solubility in aqueous media. Soluble dye (acidic or anionic, basic or cationic, direct, reactive) and insoluble dye (sulfur, vat, disperse, pigments) are two major categories in this class. About 8000 chemically distinct synthetic dyes are listed in the Colour Index (C.I.) under 40,000 trade names (Yuan et al. 2020). They are identified under a code name representing their class, colour, and

Table 2.1 Classification and example of various dyes (Javaid et al. 2021)

Types of dye	Description	Fibres applied to	Typical fixation (%)	Example	References
Acid or anionic dye	Water-soluble anionic dye, usually have –OH, –COOH, $–SO_3H$ functional group	Wool, polyamide, silk, leather	80–93	Picric acid, mauritius yellow	Lam et al. (2012)
Basic or cationic dye	Water-soluble anionic dye, brilliant colours,	Cotton, wool, acrylic	97–98	Methylene blue, malachite green	Benkhaya et al. (2020)
Reactive dye	Water-soluble, excellent fastness property, largest dye class	Cotton, cellulose, wool	60–90	Reactive red 3, reactive blue 19	Lewis (2011)
Direct Days	Water soluble anionic dyes, second largest class of dye, no need of affixing agent, cheapest price	Cotton, rayon, other cellulosic	70–95	Congo red, directive blue 1	Benkhaya et al. (2020)
Vat	Water insoluble, better colourfastness and excellent brightness, expensive dyes	Cotton, linen, other cellulosic	80–95	Indigo	Benkhaya et al. (2020)
Sulfur	Water insoluble, mostly have S-containing heterocycles, cheaper and easy to apply	Cotton, cellulosic fibres	60–70	Leuco sulfur black 1	Benkhaya et al. (2020)
Disperse	Water insoluble, non-ionic dye	Polyester, cellulose acetate	80–92	Disperse yellow 42, disperse blue 6	Benkhaya et al. (2020)
Pigment	Water insoluble, do not contain any functional group, most are benzoic derivatives and metal derivatives Used in printing			Prussian blue	Es-sahbany et al. (2018)

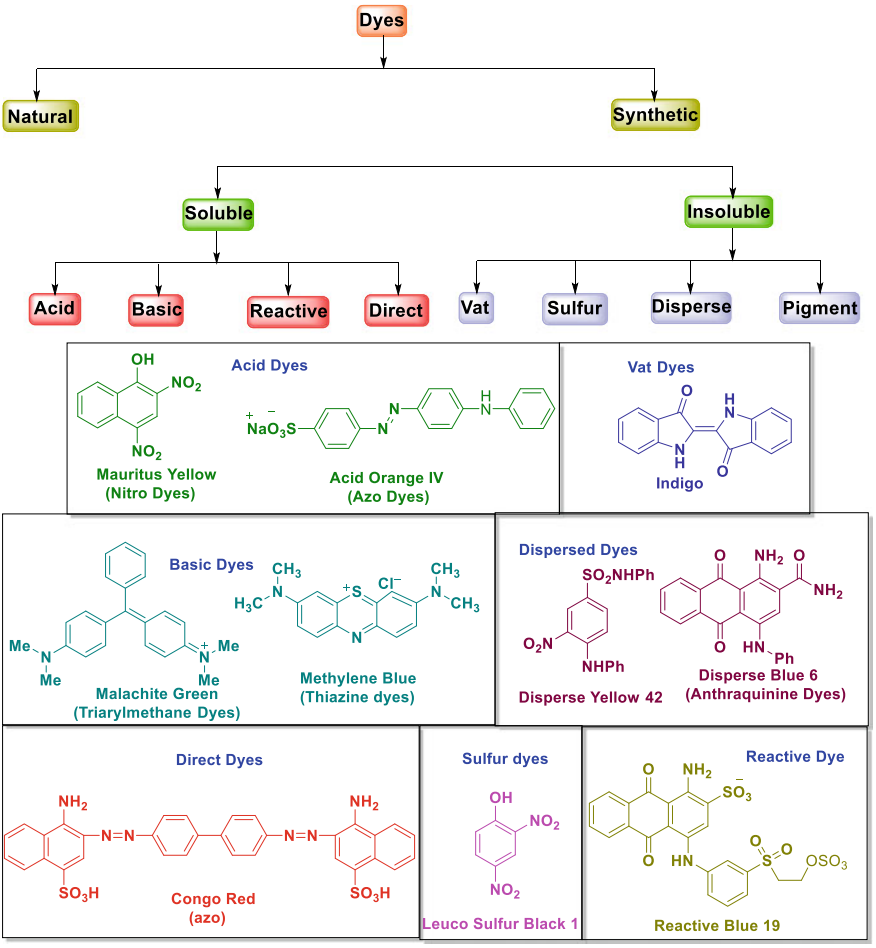

Fig. 2.2 Classification and chemical structure of dyes

order number. A general classification of dyes and chemical structure is represented in Fig. 2.2 to gain some idea of classification (Dahiya and Patel 2021).

2.3 Impact of Textile Dyes on the Environment

Dyes are referred to as recalcitrant pollutants as they are complex chemical substances and less biodegradable, persistent in the environment for a longer duration and eventually transmitted widely within diverse geographical regions. Higher stability, toxicity, high molecular mass and the presence of unusual bonds are some characteristic

features of these recalcitrant. The toxicity of a dye is due to its structure rather than the dyeing process.

Organic wastes from textile industries contain a huge amount of coloured material and are released into nearby water bodies without any appropriate treatment causing major environmental pollution. Over usage of dyes increases the toxicity of the entire ecosystem. Dye material increases pH, and BOD and COD in the released water bodies (Solís et al. 2012). Many coloured substances reduce the photosynthetic ability in aquatic plants, affect protozoa colonization and the aquatic ecosystem. The by-products of the bio treatment of azo dyes are some amines that may be harmful, carcinogenic, and more toxic than the original dye (Franca 2020). Acute toxicity involves oral ingestion and inhalation which creates problems like skin irritation and skin sensitization. Reactive dyes can cause respiratory trouble and allergic reactions in workers on occupational exposure (Tkaczyk et al. 2020). Heavy metal-containing dyes harm aquatic organisms as well as human health. These dyes produce heavy metal cations in the aquatic ecosystem which is deposited in fish gills and ultimately enter the human food chain (Ito et al. 2016). This affects human organs with a series of pathogens. Chromium-containing dyes are highly carcinogenic and impair the growth and development of plants. Apart from being carcinogenic for humans, synthetic dyes cause skin disease and affect the central nervous system. For example, 2-naphthylamine, Azure-B are known to cause bladder cancer, mutagenic disorders by interacting with DNA and RNA respectively (Khan and Malik 2018; Haq et al. 2018).

The risk associated with synthetic dye can be minimized by avoiding exposure to dry dye. Increasing the application of liquid dyes, low-dusting formulations, and using appropriate personal protective equipment are some preventive measures, and the best of them is the use of proper degradation technology of synthetic dye. The rest of the chapter is devoted to photocatalytic degradation and removal of these synthetic dyes from wastewater and soil.

2.4 Principle of Photocatalysis and Mechanistic Pathways

As described earlier, various techniques are employed for the degradation and removal of organic dyes. The AOPs are the most popular and frequently used technique amongst them. AOPs have been reported to be operative for the degradation of soluble organic pollutants from water and soils and can provide almost total degradation. The AOPs include the following techniques.

i. photolysis (UV or visible)
ii. hydrogen peroxide (include Fenton-like-reagent: $H_2O_2 + Fe^{2+}/Fe^{3+}$)
iii. ozonation/photoozonation
iv. photocatalysis (include heterogenous photocatalysis).

The photocatalytic degradation of dye using heterogeneous catalysts is the main focus of this chapter.

2.4.1 Photocatalysts

Photocatalysts harness solar energy for the PD of organic contaminants which makes the photocatalysis treatment process to be economically feasible. Photocatalysts mostly consisted of chemically stable semiconductors with a specific characteristic of sensitizers for a photocatalytic redox reaction. In a semiconductor, the bandgap (E_g) separates the lowest occupied (valence band, VB) from the highest unoccupied (conduction band, CB) energy bands. Semiconductors should be photoactive, chemo-stable, photo-stable, biologically and chemically inert, recyclable, high activity in the UV–vis region and inexpensive. The bandgap energy, irradiation wavelengths, and adsorption of a species under light determine the photocatalytic activities of a semiconductor. Thus, a semiconductor with a large bandgap absorbs in the UV region whilst a smaller bandgap semiconductor can perform a better photocatalytic activity in the visible light region. Though catalysts possess active sites for catalytic conversion, the use of the active site may not be appropriate for photocatalyst since the reaction activity of these sites is dependent on the light source. It is the preferential defects in the crystal of catalyst which act as active sites (Zhang and Jaroniec 2017).

The large numbers of reported photocatalysts can be categorized in the family of metal-oxides, metal-nitrides, metal-sulfides, and also from metal-free components like graphenes or polymers. Inorganic semiconductors have achieved a lot of success in the field of photocatalysts. Herein, the principle of photocatalytic activity of metal oxides shall be discussed mainly. Different metal oxides like TiO_2, ZnO, ZrO_2, Fe_2O_3, SnO_2, MgO, Sb_2O_3, GeO_2, V_2O_5, Cu_2O, In_2O_3, Nb_2O_5, and perovskites are the most studied materials for photocatalytic dye degradation. Photocatalytic activity of TiO_2 and ZnO has been known since 1970. Photocatalytic activity of other oxides like Fe_2O_3, ZrO_2, MgO, SnO_2, GeO_2, Sb_2O_3, V_2O_5 though known from the 70s yet their photocatalytic activity is weak. Since then, TiO_2 and ZnO have attracted the research community because of their high photocatalytic activity, non- or low toxicity, good chemical stability, inexpensive, and more or less long-term photo durability. However, the lack of activity of these catalysts in the visible spectrum is one of the main concerns.

2.4.2 Basic Principle of Photocatalysis

Different experimental techniques of dye degradation are analysed by various instrumental methods such as GC/MS, UV–vis spectrometry, ion chromatography, HPLC, capillary electrophoresis, radiometry, etc. (Rauf and Ashraf 2009). During PD, the ultimate fate of the dye molecules is to break down into smaller molecules like H_2O,

CO_2, etc. So the evaluation of total organic carbon (TOC) of the system under investigation is very important (Tanaka et al. 2000). Vigorously stirred batch photochemical cells, glass dishes, cylindrical flasks or vessels are some typical laboratory-scale experimental setups (Wu et al. 2006).

Inexpensive semiconductors as a catalyst and easy mineralization of various organic compounds have proven photocatalysis as one of the promising AOP technologies. The basic mechanism of PD consists of the following steps. When light having photon energy equivalent to or greater than the bandgap of semiconductor strikes on the surface, an electron from the valence band of the catalyst is promoted to the conduction band. This results in the generation of electron–hole pairs.

Photoexcitation:

$$\text{Catalyst} + h\nu \rightarrow e^-(CB) + h^+(VB) \tag{2.1}$$

Here e^-(CB) and h^+(VB) represent electrons in the conduction band and hole in the valence band respectively. These species can migrate to the surface of the catalyst and may undergo redox reactions with other species on the surface.

Trapping of electrons on the surface:

$$e^-(CB) \rightarrow e^-(TR) \tag{2.2}$$

Trapping of holes:

$$h^+(VB) \rightarrow h^+(TR) \tag{2.3}$$

$e^-(TR)$ and $h^+(TR)$ indicate surface trapped CB electron and VB hole respectively. In most cases, $h^+(TR)$ reacts with the surface-bound H_2O and produces hydroxyl radical. On the other hand, electron in the conduction band $e^-(TR)$ can react with the dissolved O_2 to form superoxide radical anion of oxygen, $O_2^{\bullet -}$.

Oxidation of water:

$$H_2O + h^+(\text{VB}) \rightarrow OH^\bullet \tag{2.4}$$

Photoexcited electron scavenging:

$$O_2 + e^-(\text{CB}) \rightarrow O_2^- \tag{2.5}$$

However, the activity of these two steps {steps (2.4) and (2.5)} or the activity of the photocatalytic process is reduced by the recombination of trapped carriers. This recombination of electrons and holes should be delayed so that they take part in the redox reaction. Recombination of electrons and holes takes place in the absence of oxygen, as the latter captures electrons to form a superoxide radical anion.

Charge carrier recombination:

$$e^-(TR) + h^+(\text{VB}) \rightarrow e^-(\text{CB}) + \Delta \tag{2.6}$$

The $OH^{\bullet}$ produced in step (2.4) is the most powerful oxidizing agent and reduces dye into intermediate compounds. The same reaction is repeated till all dye molecules are degraded into CO_2 and water and eventually colour fades away. This reduction reaction is more feasible in the organic medium than in water. A higher concentration of organic matter increases the number of positive holes. This enhances photocatalytic activity by reducing the electron–hole recombination (Chen et al. 2017).

Photodegradation by OH radicals:

$$OH^{\bullet} + \text{dye} \rightarrow \text{dye}_{ox} \quad (k = 10^9 - 10^{10} M^{-1} s^{-1}) \tag{2.7}$$

On the other hand, the superoxide radicals decompose pollutants by undergoing a series of reactions to produce hydrogen peroxide, hydroxy radicals, and hydroperoxyl radical anions as shown in the following reactions.

Protonation of superoxide anion radical:

$$O_2^{\bullet -} + H^+ \rightarrow HOO^{\bullet} \tag{2.8}$$

Recombination of electron–hole pairs:

$$\begin{aligned} HOO^{\bullet} + e^-(CB) &\rightarrow HO_2^{\bullet -} \\ HOO^{\bullet} + h^+(VB) &\rightarrow H_2O_2 \end{aligned} \tag{2.9}$$

A schematic presentation of the above mechanism is shown in Fig. 2.3. The overall steps of the mechanism of mineralization of dye can be summarized in the following steps (Ahmed and Haider 2018).

(i) Mass of the organic pollutants is loaded on the surface of the photocatalyst from the bulk liquid phase
(ii) Active sites of the photocatalyst adsorb the pollutant

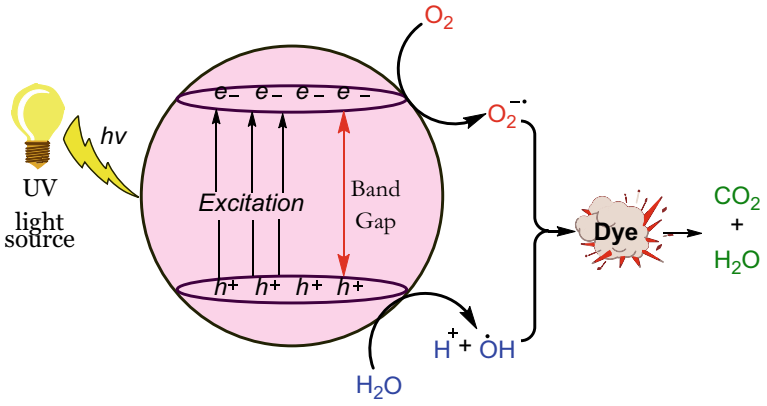

Fig. 2.3 Schematic representation of PD of dye by a photocatalyst

(iii) Hydroxyl radical ($OH^{\bullet}$) and superoxide anion radical ($O_2^{\bullet -}$) generated degrade the pollutants
(iv) The final product is detached from the catalyst surface
(v) Mass of the final product is transferred into the bulk liquid phase.

Direct (or Type-I) and indirect (or Type-II) are two suggested mechanisms for photocatalytic degradation of dyes which are discussed below.

2.4.2.1 Direct (or Type-I) Mechanisms

According to this mechanism, photoexcitation of the catalyst produces electrons and holes. The light-generated electron and hole are then captured by the dye molecules which are already chemisorbed on the catalyst surface. This results in the excitation of dye molecules (Dye*) which finally decay by the combination with the electrons. During the process, the excited electron is captured by some oxidant which enables completion of the photocatalytic cycle. Dye sensitization increases the photocatalytic activity (as it offers an expansion of the light absorption region into visible light), enhances excitation efficiency, and helps in charge separation leading to the modification of the photocatalysts (Zhao et al. 2005). The Langmuir–Hinshelwood process and the Eley–Rideal are two processes that can explain this mechanism. The former process states that electrons and holes are chemisorbed by the adsorbed dye whilst according to the later process it is the surface defects (S), that act as active centres. The degradation process as suggested by the Eley–Rideal process is shown below (Prihod'ko and Soboleva 2013).

$$\text{Catalyst} + h\nu \rightarrow e^- + h^+ (\text{generation of charge carriers}) \tag{2.10}$$

$$\text{S} + h^+ \rightarrow \text{S}^+ (\text{trapping of hole by surface defects}) \tag{2.11}$$

$$\text{S}^+ + e^- \rightarrow \text{S} (\text{decay of active centres}) \tag{2.12}$$

$$\text{S}^+ + \text{Dye}^+ \rightarrow (\text{S} - \text{Dye})^+ (\text{chemisorption of S on dye}) \tag{2.13}$$

$$(\text{S} - \text{Dye})^+ \rightarrow \text{S} + \text{CO}_2 + \text{H}_2\text{O} + (\text{degradation of dye}) \tag{2.14}$$

2.4.2.2 Indirect (or Type-II) Mechanism

In this mechanism, upon absorption of UV light by the photocatalyst, electrons from the VB are promoted to CB, creating holes in the VB. In the next phase, the photogenerated electrons and holes participate in the redox reaction on the surface

of the catalyst. Holes are trapped by water molecules giving $OH^{\bullet}$ and H^{+} whilst electrons form $O_2^{\bullet-}$ by reacting with oxygen in the medium. The reactive hydroxyl radical ($OH^{\bullet}$) and oxygen radical anion ($O_2^{\bullet-}$) finally decompose the dyes into CO_2 and H_2O.

There is an alternative mechanism for degradation in which dye molecules get self-photosensitized leading to photolysis of the dyes. The photolysis process is dominant in the natural environment but this is inefficient in removing organic pollutants from the wastewater (Zhang and Zhang 2020; Pingmuang et al. 2017). The dye molecules get excited to the triplet excited state by absorption of light. The energy released in this process excites the ground state oxygen into the first excited state which eventually oxidizes dye molecules. The $OH^{\bullet}$ and $O_2^{\bullet-}$ generated in this process are very reactive which is essential for dye degradation. Methyl Orange (MB) degrades in the natural environment via this process. However, N groups containing dye like Rhodamine B (RhB) are resistant to photolysis and undergo anaerobic photodegradation leading to carcinogenic products (Lakshmi Prasanna and Rajagopalan 2016).

2.5 Effect of Key Operational Parameters

Lately, scientists have put lots of effort to study the key operational parameters that affect photodegradation. The primary motive of all these studies is to obtain some optimum and effective conditions that are best for photo-degradation of organic pollutants. Factors like catalyst loading, exposure duration, pH, oxidizing agent, and temperature can influence the rate of PD. The effect of these factors is explained by taking TiO_2, ZnO, and some other commonly used catalysts as a reference which is discussed below.

2.5.1 Effect of pH

Evaluation of the effect of pH on photocatalytic dye degradation is a challenging task. The complication arises from different degradation reaction mechanisms for each dye. The pH of the solution is considered as one of the essential parameters owing to its impact on the performance of photocatalysts. The pH of the discharged effluent controls the surface charge of photocatalysts and influences its oxidation potential. The pH also determines electrostatic interaction between catalysts surface, substrates, and radicals during the degradation process. The separation of the photo-generated electrons and holes, surface charge, and aggregation of the catalysts are pH-dependent (Zangeneh et al. 2015). When the pH is raised beyond the isoelectic point (pH_{pzc}) of the photocatalyst, its surface acquires a negative charge. At a lower pH, the functional groups get protonated and increase the surface charge of the catalyst. Above pH_{pzc}, cationic molecules get adsorbed on the surface of the photocatalyst which is negatively charged at this pH. The reverse occurs at lower pH as anionic

Table 2.2 Optimum pH for different photocatalysts and organic dyes (Gnanaprakasam et al. 2015)

Light source	Initial concentration	Catalyst used	Organic pollutant	Optimum pH	Irradiation time (min)	Degradation efficiency (%)
UV light	200 mg/l (COD)	TiO_2	Coking water	7	60	30
100 W mercury lamp	50 ppm	Codoped TiO_2	2-Chlorophenol	12	180	95
UV light	1.2×10^{-4} M	TiO_2 and cement	Reactive yellow dye 17	5–7	480	85
40 W fluorescent lamp	6×10^{-6} M	$MnWO_4$	Methyl orange	9	480	50

molecules are easily attracted by positively charged photocatalysts (Li et al. 2020). The photodegradation mechanism has the following three important steps which can be influenced by the pH of the solution: (i) attack by hydroxyl radical, (ii) direct oxidation by the positive hole, and (iii) reduction by the valence band electron. The contribution of each step is determinant to the functional group of the substrates and pH. Though higher pH increases the hydroxyl ion concentration yet higher pH is not suitable for PD of dye because it competes with the organic molecules for getting adsorbed on the photocatalyst surface (Rajabi et al. 2013). In contrast, lower pH reduces adsorption of cationic organic dyes, therefore, reduces the efficiency of the PD in acidic media (Vinu et al. 2010). Hence, for degradation of different organic pollutants, there should be some optimum pH using photocatalyst and the same is focussed in Table 2.2. The discharge effluents of various industries are released at different pH so their effect on the PD is needed to be necessarily scrutinized (Saeed et al. 2015).

Being an amphoteric photocatalyst TiO_2 can develop both positive and negative charges on its surface. Thus, variation in the pH can affect the adsorption of dye molecules on the TiO_2 surface and thereby causing an impact on the PD reaction rate (Wang et al. 2008). Protonated and deprotonated form of titania under acidic and basic condition respectively proceeds as outlined below:

$$TiOH + H^+ \rightarrow TiOH_2^+ \tag{2.15}$$

$$TiOH + OH^- \rightarrow TiO^- + H_2O \tag{2.16}$$

Thus, the surface of the TiO_2 catalyst is positively charged in acidic conditions (or in lower pH) and negatively charged in the basic medium (or in higher pH). Reports suggest that titanium dioxide has higher oxidizing activity in acidic medium or lower pH. However, a very higher H^+ concentration slows down the reaction rate. The optimum pH for Acid Yellow 17, an acidic dye is 3 whilst Orange II and Amido

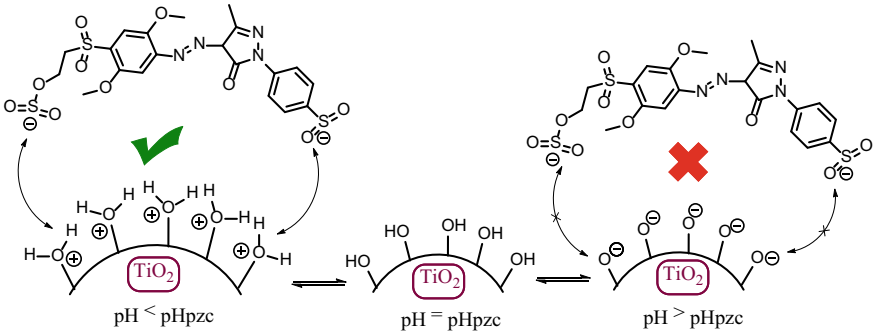

Fig. 2.4 Electrostatic interaction between RY17 and TiO_2 as a function of pH

Black 10B has shown efficient degradation at pH 9 (Behnajady et al. 2004; Qamar et al. 2004). It is reported that due to the cationic nature of Methylene Blue (MB), adsorption enhances at higher pH resulted in the high efficiency of photocatalytic degradation (Saeed et al. 2015). Anionic dye, Methyl Orange (MO) is more efficiently photodegraded in the acidic medium than in the basic medium. Research suggests that the optimal pH for MO photodegradation is 2. It is found that at this optimal pH, MO is photodegraded with complete efficiency in 20 min whilst in the basic medium no photodegradation was observed even if the exposure time is raised to 1 h. The negatively charged sulfonate groups of MO dye strongly interact with the positively charged surface of the catalyst in an acidic medium which enhances the PD of MO dye in an acidic medium compared to the basic medium. In 2017, Alahiane et al. studied the degradation of anionic Reactive Yellow-17 (RY17) dye on TiO_2 catalyst surface. The pH of zero-point charge (pH_{pzc}) for TiO_2 is 6.3. Thus, below pH_{pzc}, the TiO_2 surface acquires a positive charge which is shown by the attraction of the skeleton of negatively charged RY17 dye by the catalyst surface. Thus, dye molecules get concentrated on the catalyst surface which leads to efficient PD at pH 3. On the contrary, electrostatic repulsion between the negatively charged dye molecules and the negative charge of the catalyst surface above pH_{pzc} delays the accumulation of the dye molecules resulting in lower PD activity as proposed in Fig. 2.4 (Alahiane et al. 2017).

2.5.2 *Effect of the Dose of Semiconductor*

The efficiency of the PD process is highly dependent on the photocatalyst dosages. An increase in the photocatalyst dosages increases the dye degradation. Catalyst surface area increases with the increase in the amount of catalyst dosages/loading. A large surface area means the number of available active sites is higher leading to the formation of more $OH^{\bullet}$ *radicals, which are involved in the dye degradation. However, this positive correlation between semiconductor dosage and efficiency of*

dye degradation is limited up to certain semiconductor concentrations. Beyond the optimum amount of the catalyst, the rate constant for the mineralization of the dye diminishes. Again, this optimum amount of the catalyst is different for different catalysts and determined by the nature of the catalyst, types of contaminants and the operating conditions.

In 2019, López-Ramón et al. *evaluated the concentration effect of a nickel organic xerogel (X-Ni) as photocatalyst in the degradation of the herbicide diuron (DRN) in the aqueous phase. They varied the concentration of X-Ni photocatalyst from 100 to 5000 mg/L, the results explained that the degradation rate for constant initial DRN concentration increases with an increase in the X-Ni concentration and reaches the maximum in the 4167–5000 mg/L concentration range of the photocatalyst* (López-Ramón et al. 2019). *Further, an increase in the concentration to 5000 mg/Ls hows no improvement in the degradation rate. This effect of the catalyst concentration can be understood as the surface area and the active catalyst sites increase with the increase in the catalyst concentration up to a certain limiting concentration of the catalyst. However, above 5000 mg/L of xerogel concentration, catalyst agglomeration starts which leads to the decrease in the concentration of active sites of the catalyst for light absorption. Excess concentration of the catalyst turned the solution turbid and increase light dispersion resulting in the lower light penetration for effective degradation (*Fenoll et al. 2013*). The narrower bandgap of CdS semiconductors compared to TiO_2 makes them better photocatalysts under visible light irradiation.* The nanocomposites of CdS on graphene support make the former even better photocatalyst due to retardation in the charge recombination rate. Lu et al. in (2014) studied the effect of loading amount of this catalyst system for the photodegradation of Rhodamine B (RhB) under visible light irradiation recorded at 270 min. The report suggests that the photodegradation of RhB keeps increasing from 4 to 20 mg of the catalyst and after which it becomes constant (Lü et al. 2014). Similar trends were obtained when methylene blue (MB) is photodegraded on the TiO_2catalyst surface (Zhang et al. 2002). The effect of catalyst loading on the degradation of the dyes Reactive Red 2(RR2), Reactive Blue 4 (RB4), and Reactive Yellow 17 (RY17) was further examined by Neppolian et al. by taking TiO_2 as a catalyst. They varied the catalyst loading from 100 to 600 mg/100 mL of the dye solution. Results showed that the PD rate increases rapidly with an increase in the amount of TiO_2 up to 300 mg/100 mL for all three types of dyes. Beyond 300 mg of TiO_2, RR2 and RB4 dyes show only a slight increase in the degradation rate but for RY17, percentage degradation was found to be almost constant and rather decreases for catalyst loading 500–600 mg/100 mL. This is attributed to a decrease in the photoactivated volume of the suspension with an increase in the catalyst loading (Neppolian et al. 2002).

2.5.3 Effect of the Initial Concentration of Dye

The optimal dye concentration for better photodegradation of various dyes is needed to be considered carefully. Depending upon the initial concentration the irradiation

time needs to be adjusted accordingly to arrive at appropriate degradation under standard operating conditions. The adsorption of the dye molecules on the surface of the catalyst is dependent on the nature of the photocatalyst and functional groups present in the dyes. In general, the rate of photodegradation is higher at a lower initial dye concentration. The rate rises to a certain dye concentration and then starts falling. Increasing dye concentration would lead to more adsorption of dye molecules on the surface of the photocatalyst, thus decreasing the light penetration to the catalyst surface. The dye molecules would compete for the absorption of UV radiation with the photocatalyst. The collision frequency between the dye molecules and the active sites is higher at low initial dye concentration. The path length of the photons reaching the photocatalyst surface also increases when dye concentration is increased. Therefore, following Beer-Lambert law, this will lower the photon adsorption on the catalyst surface and eventually lowers the kinetics of PD. Haile Hassena in 2016 studied the effect of initial concentration of Methylene Blue (MB) using Al_2O_3/Fe_3O_4 semiconductor. The concentration of MB was varied from 0.5×10^{-5} to 1.4×10^{-5} M and it is observed that PD efficiency starts decreasing beyond 1.1×10^{-5} M of MB after 90 min. As more active sites are available for the cationic MB dye at low concentration, PD increases. But at higher MB concentrations, more and more molecules of MB dye get adsorbed on the Al_2O_3/Fe_3O_4 catalyst surface thus, reduces the efficiency of photogeneration of $OH^{\bullet}$ (Hassena 2016). Research conducted by Kiran et al. in (2016) explained that the rate of PD of methyl orange (MO) using Mg-doped titania under visible light raises upto 10 mg/L and then starts decreasing (Kiran et al. 2016). In (2017), Zada et al. studied the degradation of Malachite Green using bimetallic zinc and manganese oxides nanoparticles (Zn-Mn NPs). The report suggests that the percentage degradation is inversely affected by the dye concentration and about 88.41%, 80.95%, and 55.43% dye degraded in 12.5, 25, and 50 ppm dosage respectively (Zada et al. 2017). In (2019), Babu et al. examined the effect of initial dye concentration of MO in an ultrasound-assisted photo catalytic degradation. They tested the MO dye degradation by varying initial dye degradation from 0.01 to 0.04 mM in presence of CuO-TiO_2/rGO photocatalyst amount (1.0 gL^{-1}) under the mentioned technique. Results obtained from this study suggested that 98% dye degradation is obtained irrespective of initial dye concentration in 90 min through the present technique (Babu et al. 2019).

The photodegradation of dyes is dependent on the concentration of $OH^{\bullet}$ radicals on the surface of the photocatalyst and their interaction with dye molecules. At initially low concentration, the chances of collision between the dyes and the free radical are less. However, beyond the optimized concentration, the collision rate decreases due to the fewer availability of active sites resulting in the decrease of the degradation rate. As the concentration of dye increases, more dye molecules get adsorbed on the catalyst surface making the photogeneration of hydroxy radicals difficult. Degradation efficiency is not enhanced further as active sites and hydroxyl radical concentration remain constant even at higher substrate concentrations.

2.5.4 *Effect of Additives*

In dye manufacturing, some inorganic ions are usually added to the dye solution as ionic compounds make the industrial process feasible. However, inorganic ions like Fe^{2+}, Ag^{+}, Zn^{2+}, Na^{+}, Cl^{-}, $SO_4{}^{2-}$, BrO^{3-}, $PO_4{}^{3-}$, $CO_3{}^{2-}$, HCO^{3-} and persulphate ions; which are an integral part of the effluent have a diminishing effect on the dye degradation in the solution. *As a result, different additives are added during PD to increase the efficiency of the process. These additives are some oxidants like* H_2O_2 *which enhance the degradation efficiency and reduce the reaction time.*

The addition of H_2O_2 can increase the concentration of $OH^{\bullet}$ *and its ability to trap electrons make PD more efficient. Rahmat* et al. *described the role of* H_2O_2 as an initiator in the degradation of crystal violet in the presence of MnO_2-based nanofibrous mesh (MnO_2/NF) (Rahmat et al. 2019). They took 0.04 mL of H_2O_2 and measured the absorption spectra to check its impact within 1.5 h. Lowering in the absorption peak indicated the degradation of the dye. It is found that efficient degradation was obtained in 280 min in the absence of the initiator whilst the presence of the initiator reduced the timing to 60 min. As an electron capturer, H_2O_2 generates $OH^{\bullet}$ under irradiation of visible light and thus initiates the photocatalytic chain reaction (Lin et al. 2014). At optimal H_2O_2 concentration, it inhibits the complex effect of photo-generated electron hole-pairs. How H_2O_2 helps in the degradation of the dye is shown in the reaction *below:*

$$OH^{\bullet} + H_2O_2 \rightarrow H_2O + HO_2^{\bullet} \tag{2.17}$$

$$OH^{\bullet} + HO_2^{\bullet} \rightarrow O_2 + H_2O \tag{2.18}$$

$$OH^{\bullet} + OH^{\bullet} \rightarrow H_2O_2 \tag{2.19}$$

For the detection of the main species in the PD of dyes, various researchers add scavengers to the photocatalytic reaction condition. A thorough examination of these species and their way of generation and utilization in dye degradation is a matter of prime importance in the photocatalysis study. Alcohols, *p*-benzoquinone, EDTA-2Na, and Ar gas, $AgNO_3$, KI are some frequently used scavengers. Daneshvar et al. examined the effect of radicals in the PD of Acid Red 14 dye using TiO_2 suspension under irradiation of UV-C lamp (30 W) (Daneshvar et al. 2003). They used ethanol to quench the hydroxy radical. Upon addition of 0.02% (v/v) of quencher, the PD efficiency reduced to 12.4% after exposing for 2 h but the degradation did not stop completely. This indicates that hydroxy radicals are not the only ones that assist in the degradation. Positive holes h^{+}(VB) formed on the irradiated photocatalyst which reacts with the adsorbed dye, may assist in the degradation.

As explained above, ions have a diminishing effect on photocatalytic dye degradation. The effect of these ions on the reduction of degradation efficiency is explained below based on their chemical reactions in solutions. For example, the presence of

Fe^{2+} ion easily converted $OH^{\bullet}$ to OH^{-} and thus decrease the concentration of $OH^{\bullet}$ in the reaction medium. This eventually leads to a decrease in the dye degradation (Yoon et al. 2001).

$$OH^{\bullet} + Fe^{2+} \rightarrow OH^{-} + Fe^{3+} \quad (k = 3.5 \times 10^{8}\, M^{-1}s^{-1}) \tag{2.20}$$

Likewise, the other ions such as CO_3^{2-}, HCO_3^{-} *which are added to the dye bath for maintaining pH eventually have a negative impact on the dye degradation. The presence of these ions scavenges the* $OH^{\bullet}$ *radicals and causes a percentage decrease in the PD. The presence of oxygen or air also influences the degradation efficiency. Oxygen molecules scavenge CB electrons and this leads to an increase in the production of active oxygen species such as* H_2O_2, $O_2^{\bullet-}$, $HOO^{\bullet}$, and $OH^{\bullet}$. This helps the catalysts to restore their original form and thus completes the catalytic cycle (Zhao et al. 2005).

2.5.5 Effect of Temperature

The influence of experimental temperature conditions on the efficiency of degradation of organic dyes by photocatalysts has been less investigated. Zazo et al. in (2011) *reported that the decomposition efficiency of phenolic dyes using Fenton oxidation is almost 80% at 120* °C *which is reduced to 28% on decreasing the experimental temperature to 25* °C (Zhao et al. 2005). *Salem et al. examined the influence of temperature on the photodegradation efficiency of Acid Blue 29 (AB29) using* MMTK10-Cu(en)$_2$ as the catalyst. They varied temperatures in the range of 20–40 °C. *The decolouration efficiency was raised from 51.8 to 88.2% on rising the experimental temperature from 20 to 40* °C *when irradiated for 18 min* (Salem et al. 2014). *Javaid et al. studied the total organic carbon (TOC) removal of* Remazol Brilliant Blue R (RBBR). Keeping the initial dye concentration at 20 ppm, pressure 10 MPa, and using a continuous-flow tubular reactor coated with a thin layer of PdO as a catalyst they increased the temperature from 200 to 250 °C and finally to 300 °C. The catalytic efficiency likewise increased from 89 to 92% and 99.9% respectively (Javaid et al. 2016). Thus, a rise in temperature increases the degradation efficiency. Higher temperature pushes the degradation reaction forward by overcoming electron–hole recombination and generating more free radicals by bubble formation in the solution. Additionally, an increase in the experimental temperature helps in the rapid oxidation of organic dyes at the interface (Vinu et al. 2010).

2.5.6 Effect of Light Intensity and Wavelength

Being a photocatalytic process, light has a critical role in the PD of organic dyes. The rate and the efficiency of the PD process are proportional to the intensity of the

used light. As stated by Ollis et al. the rate of PD is first order if the light intensity is between 0 and 20 mW/cm^2 and varies linearly with increasing light intensity. At intermediate light intensities, the PD rate is proportional to the square root of the light intensities. Thus, follows half order kinetics at intermediate intensities. However, PD is independent of light intensities for the highly intense light sources. At high light intensity photons per unit time and unit area increases resulting in stronger photocatalytic activity. Though light intensity increases, the number of active sites remains the same on the catalyst surface and hence the reaction rate remains constant after reaching an optimum light intensity (Ollis et al. 1991).

The undesired electron–hole recombination is high when irradiated at high intensity, leading to a decrease in the PD rate of the dye. Muruganandham and Swaminathan investigated the effect of light intensity on the decolouration and degradation of azo dye Reactive Yellow 14 (RY14) using a TiO_2-UV system (Muruganandham and Swaminathan 2006). Their results explained that the decolouration of dyes increases to 87.9% from 35.9 when light intensity is enhanced from 16 to 62 W in 20 min time. Similarly, the degradation of dyes also increases from 26.5 to 59.4% in the same duration. The photooxidation increases linearly between 16 and 32 W and from 32 to 48 W no insignificant improvement in photooxidation was observed (Ollis et al. 1991). However, beyond 48 W, the photooxidation is independent of the light intensity. The optimum photooxidation was achieved at 32 W UV light. Though solar and UV lights are used for PD, yet artificial (UV) light is dominating in this field. Because of the constant stable source of light intensities irrespective of the weather and other environmental factors, artificial light sources are preferred. Moreover, the higher efficiency of UV light in PD over solar irradiation makes them more useful. However, the higher abundance, easy accessibility, and non-harmful nature of solar light make them alternative and economical light sources. Solar light consists of 5% UV light (200–400 nm), 43% visible light (400–800 nm), and more than 52% IR. The artificial UV light for its reproducible nature and high energy compared to solar irradiation found to be highly efficient in the degradation of the dyes. At higher light intensity electron–hole pairs recombination is slow thus makes the PD process faster. TiO_2 has a wide bandgap energy (3.2 eV for anatase, 3.00 eV for rutile, and 3.13 eV for brookite). The wider bandgap restricts its absorption in the UV region of the solar spectrum (Kuang et al. 2009). The photodegradation rate of dyes in the aqueous phase for TiO_2 catalysts is influenced by the intensity of UV light. Neppolian et al. investigated the effect of intensity and source of the light whilst using TiO_2 as photocatalyst and Reactive Yellow 17 (RY17), Reactive Red 2 (RR2), and Reactive Blue 4 (RB4) as dyes (Neppolian et al. 2002). Higher degradation was achieved for all three types of dyes when the intensity of solar radiation was raised.

To study the effect of different light sources Yan-fen et al. took sulforhodamine-B dye for photodegradation employing TiO_2 catalyst under three different light sources. The visible light source was 500 W halogen light with intensity 70.6×10^3 I_x, source of solar light was irradiation of sunlight between 12.00 am and 2.30 pm with corresponding intensity $(80 \pm 5) \times 10^3$ I_x and a 100 W mercury lamp was the UV light source with intensity 105×10^3 I_x. Results obtained showed that the PD rate constant with UV light is the highest and least with visible light (Yan et al. 2006).

Stengl et al. examined the wavelength dependency of PD rate in the degradation of Orange II dye in an aqueous medium using rare earth metal-doped TiO_2 as the catalyst. And explained that the degradation rate constant is affected by wavelength for the TiNd_3 catalytic system. TiNd_3 i.e., titania doped with rare earth metal Nd is found to be the best photocatalytic system for the degradation of Orange II dye under irradiation of visible light. The energy of the photon is interrelated to its wavelength and a shorter wavelength is associated with greater photon energy which is reflected in the PD rate constant. Results showed that rare-earth ion doping in titania is helpful in the visible light photocatalytic activity of TiO_2 as reflected in the redshift of the optical absorption spectrum (Štengl et al. 2009).

2.5.7 Effect of Irradiation Time

PD capacity of heterogeneous catalysts towards organic dyes has been analysed considering irradiation time. Reports suggest that PD increases with an increase in the irradiation time in photocatalytic reactions. This attributes to an increase in the formation of more $OH^{\bullet}$ and $O_2^{\bullet -}$ with irradiation time. However, the rate slows down after some optimum time. This optimum time depends on the catalysts as well as the types of dye. Sakthivel et al. used azo dye Acid Brown 14 as a model dye for the investigation of the effect of irradiation time by two different catalysts viz., ZnO and TiO_2 (Sakthivel et al 2003). As per the report, the rate of decolouration and degradation increases with an increase in the irradiation time and slows down after irradiation of light for 1 h. The reduced rate of degradation after a certain time limit is attributed to the difficulty in the oxidation of this nitrogen-containing dye. They found that when all other operating conditions were kept constant, the complete decolouration of acid Brown 14 occurred in 2 h for ZnO and 5 h for TiO_2. However, for the complete degradation, ZnO took 6 h and 7 h for TiO_2. Ramli et al. in (2014) also evaluated photocatalytic activity as a function of irradiation time in the degradation of MB under different catalysts (Ramli et al. 2014). Results explained that the rate of PD is rapid in 0–30 min for TiO_2/AC (TiO_2 with activated carbon) and TiO_2/PANi (TiO_2/Polyaniline). The rate became slower after 30 min for both the samples. However, TiO_2/AC was found to be a better catalytic system with complete degradation in 90 min. Availability of more active sites and a high rate of formation of $OH^{\bullet}$ at the starting of the degradation process is the reason behind this. The repulsive forces between the molecules on the surface with bulk phase hindered the filling of remaining active sites after a certain limiting time. Thus, the rate of degradation tends to be constant after some time.

2.6 Degradation Studies of Dyes

For the removal of toxic dyes, different types of physical, chemical, and biological techniques have been established in the last few years. Amongst all these procedures, the adsorption process is one of the utmost choices for the decolourization of dyes and various types of dissolved colouring materials. Different technologies such as UV–vis spectrophotometry (Al-Mamun et al. 2019; Alnuaimi et al. 2007), HPLC (Abdullah et al. 2007), GC/MS (Benatti et al. 2006), ion chromatography (Blanco-Galvez et al. 2007), radiometry (Dionysiou et al. 2000), X-ray diffraction (XRD) (Andronic and Duta 2007) etc. have been employed to quantify the efficiency of dye removal and characterize the fate PC. After total mineralization, most of the dyes were converted to carbon dioxide (CO_2) and water (H_2O). During degradation, nitrogen is mineralized to N_2, NH_4^+ and NO_3^- ions which depends on the initial oxidation state of nitrogen, the structural conformation of the substrate, and irradiation time. Similarly, chlorine can be transformed to chloride (Cl^-), sulfur to sulfate (SO_4^{2-}), phosphorus to phosphate (PO_4^{3-}), and so on. The extent of dye mineralization can be monitored by measuring total organic carbon (TOC) or the measurement of chemical oxygen demand (COD) and biological oxygen demand (BOD). Usually, with increasing the amount of NH_4^+, Cl^-, SO_4^{2-}, and NO_3^- the values of COD or TOC decrease with irradiation time. In general, the compounds which do not form stable intermediates at low dye concentration can complete their mineralization with half-lives for parent dye.

2.6.1 General Considerations

With the evolution of experimental techniques, several semiconductors have been used according to their effectiveness towards dye degradation, including TiO_2, V_2O_5, ZnO, WO_3, CdS, ZrO_2, and their saturated forms (Andronic and Duta 2007; Hasnat et al. 2007). Titanium dioxide (TiO_2), one of the most popular photocatalysts, has been applied to investigate dye degradation due to its non-toxicity, ready availability, and high chemical stability. Because of the large bandgap (~3.1 eV), TiO_2 is utilized under UV irradiation (250–350 nm). Later, it has been extended to hydrogen production, solar cells, pollutant photo-oxidation, and removal of dye in liquid and gaseous phases (Atarod et al. 2016).

In comparison to TiO_2, the photocatalytic efficiencies of other semiconductors such as ZrO_2 are quite dissimilar. Although the bandgap energy for both TiO_2 and ZrO_2 are the same (3.1 eV) the efficiencies of TiO_2 in the separation of photo generated charges (less e^-/h^+ recombination rate) are higher due to the structural conformation of the material. On the other hand, due to intra-bandgap surface states, ZrO_2 shows a low absorbance in UV ranges, thereby causing its low activity (Bandara et al. 2017; Reddy et al. 2018).

Due to chemical stability, inexpensive, and large absorption spectrum, ZnO has been broadly employed as a photocatalytic material for decolourization of wastewater than that of TiO_2. Methyl Orange (MO), Acid Orange (AO), and Acid Red (AR) were degraded using ZnO under UV illumination (365 nm) and the rate of degradation order of these dyes is: AR > AO > MO (Anwer et al. 2019). The significant advantage of using ZnO is its ability to absorb a large fraction of the solar spectrum compared to the other semiconducting metal oxides and the major drawbacks are its wide bandgap energy and photo corrosion. Due to wide bandgap energy, the absorption of ZnO is limited in the visible light region, resulting in fast charge carrier recombination and ultimately low photocatalytic efficiency. The optical, structural, and magnetic properties of ZnO can be improved and altered by surface modification of ZnO catalysts that had several higher defect states exhibited better dye adsorption but low photocatalytic activity (Liu et al. 2013).

2.6.2 Photocatalytic Degradation Scheme for an Azo Dye

Azo dyes constitute a significant class of synthetic and coloured organic compounds which are characterized by one or more nitrogen to nitrogen double bonds (–N=N–). The determination of the colour of azo-dyes fully depends upon the azo bonds and their associated chromophores and auxochromes. The azo bonds are much more active and can readily oxidized by positive hole or hydroxyl radical ($OH^{\bullet}$) or reduced by the electron in the conduction band (CB), thereby resulting in the cleavage of the –N=N– bonds which leads to decolourization of dyes (Rauf and Ashraf 2009). However, synthetic dyes commonly used on an industrial scale are azo (monoazo, diazo, triazo) anthraquinone, phthalocyanine, triarylmethane, and xanthene derivatives. These types of dyes are released in the aqueous streams from the effluents of various industries such as textiles, paper, leather, plastics, etc. Because of the toxicity and persistency of azo dyes, their removal from textile wastewater has become a matter of interest. Recently, conventional technologies, including primary (adsorption, flocculation), secondary (biological methods), and chemical processes (chlorination, ozonization) are used for degradation of the colour of the water with dye-contamination.

The photocatalytic degradation of aqueous solutions of Acid Orange 7 (AO7) has been analysed with the use of a solar light-irradiated TiO_2 catalyst. AO7 mainly exists in two tautomeric forms, i.e., one is the azo form and the other one is the hydrazone form. However, the hydrazone form is predominant in the aqueous solution and the photo catalytic decolouration leads to complete mineralization of the dye solution (Rauf and Ashraf 2009). AO7 absorbs on the surface of the photocatalyst via the oxygens of its hydrazone and sulfonate group. Initially, the cleavage of the dyes in the vicinity of the azo bond occurs in the presence of solar light, followed by the cleavage of attached aryl rings. This step takes place via a photosensitized mechanism, resulting in decolouration of the solution without significantly affecting the COD. The mechanism for the formation of oxidative species, following excitation

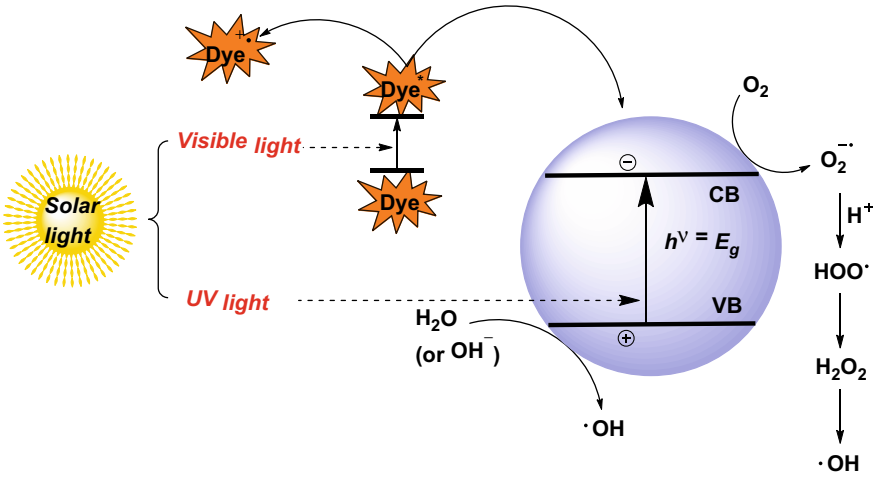

Fig. 2.5 Mechanisms of generation of oxidative species of AO7/TiO_2 system

of AO7–TiO_2 system with solar light is shown in Fig. 2.5. In this process, TiO_2 adsorbs the dye on its surface and undergoes a series of oxidation steps, which lead to decolourization and formation of several intermediates (mainly aromatic and aliphatic acids), resulting in the decrease of pH and an increase in the conductivity of the solution. Further, these molecules undergo oxidation forming low molecular weight species and, eventually, to CO_2 and inorganic ions, such SO_4^{2-}, NO_3^-, and NH_4^+ (Rauf and Ashraf 2009; Stylidi et al. 2003).

In addition to this, the degradation of several azo dyes such as Acid red 18, Methyl Orange, Remazol Black 5 (RB5), and Procion Red MX-5B has also been investigated utilizing TiO_2 photocatalyst (Tanaka et al. 2000; Sahel et al. 2007; Mozia et al. 2005). The examined dyes include both monoazo and diazo dyes and their rate of degradation can be associated with the disappearance of colour and the rate of elimination of total organic carbon (TOC). Based on this, it can be revealed that monoazo dyes are easy to degrade in comparison to diazo dyes and the majority of intermediates observed are aromatic amine, phenolic compounds, and several organic acids. Adsorption of dye on the surface of TiO_2, is one of the significant factors that measures the rate of degradation. Photocatalytic degradation of azo dye mainly proceeds through oxidation by positive hole (or $OH^{\bullet}$) and reduction by CB electron. The adsorption isotherm of RB5 dye represents an L3 type which indicates the formation of at least two layers of dye on the photocatalyst surface. With increasing the dye concentration the adsorption of MX-5B decreases. This behaviour can be described by the competition of adsorption between impurities and dye or the modification of TiO_2 charge (Sahel et al. 2007).

2.6.3 Effect of Substituents

Dyes with different substituents have a considerable effect on PD which has been investigated using an aqueous solution of TiO_2. The rate of photocatalytic degradation of azo dyes is higher compared to the dyes with anthraquinone structure. The presence of methyl ($-CH_3$) and chloro ($-Cl$) groups in dyes slightly decreases the degradation efficiency whilst the reverse is shown by the nitrite group. The side-chain alkyl groups decrease the water solubility and consequently, disfavour the process of photocatalytic degradation. The dyes having more sulfonic substituents are less reactive compared to hydroxyl-containing ones. The hydroxyl groups enhance the electron resonance in the molecule and the degradation rate of the dye. Also, photocatalytic degradation of triazine-containing azo dyes, Procion Red MX-5B and Reactive Brilliant Red K-2G, in aqueous TiO_2 dispersions revealed that decolouration and desulfuration occurred at the almost same rate in the first step of the photo-oxidation process. Dyes molecule containing naphthalene groups are hydroxylated more easily compared to the dyes having a triazine group thus, the rate of mineralization is slow for the latter. Most of the intermediates are aromatic and aliphatic carboxylic acids and oxidized slowly to CO_2. For both the dyes, the rate of mineralization is much slower in comparison to the rate of decolourization and ultimately converted to cyanuric acid a stable structure for photocatalysis (Hu et al. 2003).

Methyl substituents have an impact on photocatalytic efficiency in the degradation process. For example, between Acid Orange 7 (AO7) and Acid Orange 8 (AO8), the reactivity of AO8 is lower due to the presence of methyl ($-CH_3$) substituents (Neppolian et al. 2002). In the case of AO8, AO10, AO12, the order of the photocatalytic decolourization kinetics is AO10 > AO12 > AO8. This is attributed to the presence of two sulfonic acid groups in AO10 which helps binding the catalyst surface (Khataee and Kasiri. 2010). In the case of Acid Red 29 (AR29) and chromotrope 2B, the latter one contains a nitrite group in the *para* to the azo bond and showed a slightly higher reaction rate. The nitrite group can interact with the phenyl ring by delocalization of the π-electrons of the ring and unpaired electrons of the heteroatom which leads to favour the electrophilic attack (Qamar et al. 2004). In presence of chlorine atoms, the inductive effect ($-$I effect) largely exceeds the mesomeric effect (+M effect) and the ring is deactivated thus $OH^{\bullet}$ can easily generate Cl^- in the solution. The electronic properties of a $-$OH group are $-$I and +M effects. That is why the rate of photocatalytic decolourization of Acid Red 29 (containing two hydroxyl substituents) is higher in comparison to that of Orange G (containing one hydroxyl substituent) (Lachheb et al. 2002). Similarly, a carboxylic group also accelerates the rate of decolourization. For example, amongst Alizarin S (AS), Orange G (OG), Methyl Red (MR), and Congo Red (CR) the photocatalytic rate constant order is MR > OG $\approx$ AS > CR. This is because of the higher degradability of Methyl Red due to the presence of carboxylic group which can readily react with H^+ via a photo-Kolbe reaction (Khataee and Kasiri 2010; Lachheb et al. 2002).

2.6.4 Comparison of Cationic and Anionic Dye

In the presence of UV light and TiO_2, most of the cationic and anionic dyes are prone to photocatalytic degradation. As evaluated by colour index (C.I.) it was found that only cationic dyes are adsorbed by TiO_2, except for Quinizarin (adsorption efficiency of 21.8%) and Basic Orange 2 (no adsorption is displayed). This was explained concerning the surface structure of TiO_2. The oxygen atoms present on the surface of the unmodified crystal of TiO_2 contain a negative charge and, therefore, the cationic molecules are more readily absorbed. Thus, for cationic dyes, the highest values of photocatalytic degradation rate constant are observed and these results suggest that the adsorption hypothesis of dye has a significant effect on its susceptibility to photocatalytic degradation. However, no correlation was found between adsorption efficiency and the rate constant values of photodegradation. A linear correlation was observed between k^{-1} (inverse value of photocatalytic degradation rate constant) and the absorbance of the illuminated solution when measured at 366 nm. The surface of the photocatalyst can only adsorb cationic dyes and their photocatalytic degradation is faster in comparison to that of anionic dyes (Baran et al. 2008).

2.6.5 Correlation of Dye Degradation with Its Type

Dyes are classified mainly based on the conformational structures, sources, colours, and method of applications in the colour index, which has continuously been studied. Further, based on the chromophore, different categories of dyes have also been considered. Dyes are differentiated with respect to their core skeletonviz. acridine, azo, arylmethane, anthraquinone, nitro, xanthene, quinone-amine, etc. However, in literature, there are no examples of any correlation between percentage degradation and structure or class of dyes for PD. However, from various studies, the order of degradation is observed as follows: Auramine O > Safranin O > Malachite Green > Amido Black > Rhodamine B > Carmine, which was established using the UV/H_2O_2 photolytic AOP. The same order is also observed for other AOPs as hydroxyl radicals ($OH^{\bullet}$), responsible for the dye degradation. In general, it was revealed that diarylmethane class dyes are most effectively degraded, whereas anthraquinone class dyes are least degraded (Table 2.1).

2.6.6 Effect of Doping and Mixed Semiconductors

Doping refers to the introduction of impurities/foreign atoms into the basic structure of a parent material that can improve photocatalytic performance for dye degradation. Several metals including Pt, Li^+, Zn^{2+}, Cd^{2+}, Ag^+, Co^{3+}, Cr^{3+}, Fe^{3+}, Al^{3+}, etc. have been used as dopants (Pelaez et al. 2012; Li and Li. 2002; Su et al. 2007). Doping with

metals and non-metals is one of the promising strategies to alter the optical response of TiO_2 photocatalyst. Doping changes the bandgap energy as well as enhances the characteristics and activity of photocatalytic species under visible light. The incorporation of transition metals in TiO_2 crystal lattice may lead to form a new energy level between VB and CB, inducing a shift of light absorption towards the visible light region (Pelaez et al. 2012). Various techniques to make TiO_2 absorb photons of lower energy have been employed, including surface modification (via organic materials and semiconductor coupling), bandgap modification (by creating oxygen vacancies), and oxygen sub-stoichiometric adjustments by co-doping of non-metals and metals. The transition metal doping increases the photocatalytic activity by scavenging electrons that reduce the recombination of charges and therefore favour the $OH^{\bullet}$ formation. Doping modifies the surface properties of the material active sites due to induced defects, thus increase the adsorption and favour the interfacial reactions. Non-metals such as nitrogen, sulfur, phosphorous, fluorine, and carbon are also used as dopants (Garg et al. 2019). Nitrogen is the most promising dopant that can easily substitute oxygen in TiO_2 lattice. Due to the versatility in the structure-electronic properties and biocompatibility, metal oxides such as TiO_2, ZnO, and WO_3 are characterized by their identical bandgap excitation mechanism and the potential of VB holes to generate hydroxyl radicals. A wide range of pollutants in gas and liquid regime can be completely mineralized under light illumination conditions using these metal oxides. Co/N co-doped TiO_2 with variable dopant composition could be synthesized by wet impregnation method and used as a dopant by increasing the cobalt composition for the degradation of bisphenol-A [2,2-bis (4-hydroxyphenyl) propane]. The physical properties of the nanoparticles are disturbed by dopants like Co and N, which altered the crystal structure, energy bandgap as well as elemental composition (Garg et al. 2019).

2.7 Types of Heterogeneous Photocatalysts

Heterogeneous photocatalysis accelerates a photoreaction by chemical transformation. Semiconductors are the most important photocatalyst materials having a VB and a CB with a defined bandgap. Various kinds of applications viz., purification of water and air, water disinfection and environmental remediation can be accomplished using different semiconducting photocatalytic materials. In this context, in (1972), Fujishima and Honda discovered the photochemical splitting of water into hydrogen and oxygen in the presence of TiO_2 (Fujishima and Honda 1972). The metal oxides such as TiO_2, ZnO, Fe_2O_3, SnO_2, ZrO_2, MgO, GeO_2, Sb_2O_3, V_2O_5, Cu_2O, Nb_2O_5, and perovskites have been studied as semiconductors. The photocatalytic activity of Fe_2O_3, SnO_2, ZrO_2, MgO, CdS, or V_2O_5 was also analysed but their photocatalytic efficiencies were somewhat lesser than the TiO_2. Herein, we will focus on two well-explored photocatalysts TiO_2 and ZnO. According to their efficiencies, photocatalystsis categorized into three generations. The first generation

consists of single-components (such as TiO_2, ZnO, CdS), whilst the second generation is multiple components (such as $WO_3/NiWO_4$, $BiOI/ZnTiO_3$, C_3N_4/Ag_3VO_4) whereas, the third generation contains photocatalyst immobilized on solid substrates (e.g., FTO/WO_3-ZnO, Steel/TiO_2-WO_3, Glass/P-TiO_2) (Anwer et al. 2019).

2.7.1 TiO_2 Catalyst

Titanium dioxide is one of the most effective photocatalysts utilized in oxidation of organic pollutants due to its chemical and photochemical stability, high photoactivity, low energy consumption and biocompatibility. It can be activated under UV irradiation, forming an active oxygen species e.g., hydroxyl radicals ($OH^{\bullet}$) on the surfaces of the TiO_2 crystals. The bandgap of TiO_2 is more than 3.0 eV (~3.0 eV for rutile and ~3.2 eV for anatase), which makes it primarily active for UV light. Most of the organic dyes could be decomposed into CO_2 and H_2O by the attack of these radicals and a variety of intermediates are formed in the aqueous solution. TiO_2 can only be excited by ultraviolet light having a wavelength (λ) less than 390 nm, therefore the light utilization efficiency to solar irradiation is quite low. The photocatalytic activities of TiO_2 are being explored by upgrading the morphology of TiO_2 such as surface area, crystal composition, particle size, bandgap, porosity, and hydroxyl density on the surface (Chen et al. 2020; Luttrell et al. 2015).

The crystal structure of TiO_2 consists of three phases, anatase, rutile, and brookite (Fig. 2.6). The most common commercial photocatalyst Degussa P-25 contains both rutile and anatase crystalline forms. Due to the synergistic effect of phase mixture of different polymorphs, photocatalytic activity increases compared to pure phases. However, the pure phase anatase exhibits higher photocatalytic activity compared to rutile TiO_2. The bandgap of the anatase form of TiO_2 is larger compared to the rutile form. This reduces the light absorption and increases the valence band to a higher energy levels corresponding to redox potentials of adsorbed molecules. As a result, the oxidation power of electrons increases and facilitates electron transfer from the TiO_2 to adsorbed molecules. In addition, anatase exhibits an indirect bandgap that is smaller compared to its direct bandgap, whilst for rutile structure, the fundamental

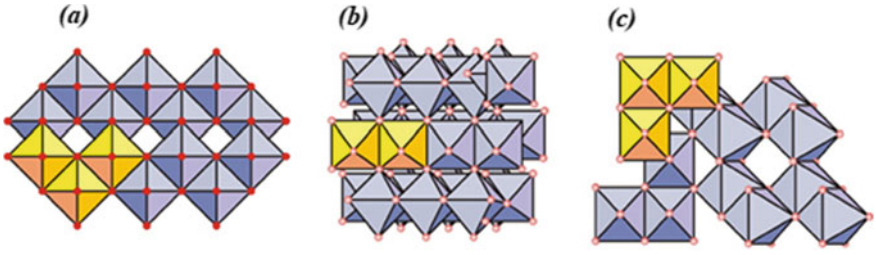

Fig. 2.6 Polymorphs of TiO_2. **a** Anatase, **b** brookite and **c** rutile (Khataee and Kasiri 2010)

bandgap is either direct or indirect bandgap which is similar to its direct bandgap. In general, the semiconductors with indirect bandgap exhibit longer charge carrier lifetimes compared to direct gap materials. Therefore, anatase with a longer electron–hole pair life is more likely to participate in surface reactions compared to the rutile (Luttrell et al. 2015).

2.7.1.1 TiO_2 Doped Photocatalyst

Photocatalytic degradation increases with an increase in the amount of dopant which can trap electrons, and initiate the reaction with water to form oxidative radicals responsible for the degradation of organic pollutants. However, too much dopants prevent the TiO_2 from capturing photons resulting in the restricted generation of electron–hole pairs thereby decreasing photocatalytic efficiency. The efficiency of TiO_2 is restricted due to its large bandgap (>3 eV), which impedes its application in photodegradation using solar light. Therefore, considerable modifications have been made to shift the absorption of TiO_2 from UV to visible light. Decrease in the bandgap of TiO_2 is the primary target of doping, i.e., to induce a bathochromic shift and extend its wavelength range correspond to visible regions. The degree of degradation of organic pollutants is caused by the single-doped and co-doped TiO_2 photocatalysts, where co-doped TiO_2 generally have higher photocatalytic activities in comparison to single-doped TiO_2. For modification of the electronic structure of TiO_2, transition metal ions, such as Pd^{2+}, Cu^{2+}, Cd^{2+}, Cr^{3+}, V^{5+}, Fe^{3+}, Ni^{2+} are investigated. This introduces donor and/or acceptor levels in the bandgap, which excites the photocatalyst even with lower energy photons and exhibits higher photocatalytic activity under visible light (Pan et al. 2010). In addition to this, the higher quantum efficiency is also responsible for dopant in TiO_2 photocatalytic reaction, as a result, it prevents from recombination of generated electron–hole pairs. Therefore, the charge transfer of electrons and holes is increased between the rutile and anatase form of TiO_2 by this mixed-phase (Lai et al. 2016). At high dopant concentration, the metal ions can behave as recombination centres for the photoinduced charge carriers, thereby decreasing the quantum efficiency. Vanadium, copper, and cobalt doping on TiO_2 offer a promising photocatalytic approach under visible light. Due to the synergistic effect, Co-doped TiO_2 generally exhibits higher visible light absorption with respect to single-doped TiO_2, as a result increasing the charge carrier lifetime. During irradiation of higher wavelengths of light, the degradation of rutile C, N, S-TiO_2 nanorods shows higher efficiency in comparison to anatase C, N, S-TiO_2 nanorods even though the latter has a higher surface area (Wang et al. 2017). This suggests that the catalyst phase is a more important factor than the surface area, which affects the co-doping catalytic activity.

2.7.1.2 Principle and Mechanistic Study of TiO_2 in Photocatalytic Reaction

The mechanism of photocatalysis can be investigated as a correlation of semiconductor solid catalyst with the light of suitable wavelength. For a photocatalyst, the electrons lie in the valance band at ambient temperature. For a favourable photocatalysed reaction, the recombination of electrons and hole must be prevented. The ultimate goal is to have a reaction between the electrons and oxidant to produce a reduced product and a similar reaction between holes and reductant to give an oxidized product. Under UV light irradiation (photons) of TiO_2, electrons and positive holes are generated in the conduction ($e_{CB}{}^{-}$) and valence band ($h_{VB}{}^{+}$) according to the Eq. 2.21 (Chen et al. 2020; Poulopoulos and Philippopoulos 2004). The holes can either react directly with organic molecules (Eq. 2.26) or form hydroxyl radicals (Eqs. 2.22and 2.23) that subsequently oxidize organic molecules (Eq. 2.27) (Ahmed et al. 2011; Akpan and Hameed 2009). The electrons can also react with organic compounds to provide reduced products (Eq. 2.28). The oxygen (Eq. 2.24) can react with electrons and reduce the dye or react with electron acceptors such as adsorbed O_2 on the surface of Ti(III) or dissolved in water, reducing it to $O_2{}^{-\bullet}$. The photogenerated holes can also oxidize the organic molecule to form R^+, or react with OH^-or H_2O and oxidize them to $OH^\bullet$. The resulting $OH^\bullet$, being a very strong oxidizing agent (standard redox potential +2.8 V) can oxidize most azo dyes to mineral endproducts (Akpan and Hameed 2009). According to this, the appropriate reactions at the semiconductor surface causing the degradation of dyes can be expressed as follows:

$$TiO_2 + h\nu(UV) \rightarrow TiO_2\left(e_{CB}^- + h_{VB}^+\right) \tag{2.21}$$

$$TiO_2\left(h_{VB}^+\right) + H_2O_{absorbed} \rightarrow TiO_2 + H^+ + OH^\bullet \tag{2.22}$$

$$TiO_2\left(h_{VB}^+\right) + OH_{surface}^- \rightarrow TiO_2 + OH^\bullet \tag{2.23}$$

$$TiO_2\left(e_{CB}^-\right) + O_{2\,absorbed} \rightarrow TiO_2 + O_2^{-\bullet} \tag{2.24}$$

$$O_2^{-\bullet} + H^+ \rightarrow HO_2 \tag{2.25}$$

$$h_{VB}^+ + \text{Organic} \rightarrow \text{Oxidation products} \tag{2.26}$$

$$OH^\bullet + \text{Organic} \rightarrow \text{Degradation products} \tag{2.27}$$

$$e_{CB}^- + \text{Organic} \rightarrow \text{Reduction products} \tag{2.28}$$

where *hv* is the energy of photon required to excite the semiconductor electron from the VB region to CB region.

2.7.2 ZnO Catalyst

ZnO is another photocatalyst that is getting increasing attention owing to its high photocatalytic activity, good stability, eco-friendly, and cost-effective nature. It is preferred over other semiconducting metal oxides as it can absorb a large fraction of the solar spectrum. Thus, ZnO has emerged as an attractive PC to remove persistent organic pollutants from wastewater. ZnO is a well-defined naturally occurring oxide having three different crystalline structures which are commonly known as rocksalt, wurtzite, cubic (zinc blende) and their structure is shown in Fig. 2.7. The rocksalt structure of ZnO is quite rare because it can be obtained under high pressure. Amongst the three structures, wurtzite form is the most common structure of ZnO and has the highest thermodynamic stability. At ambient pressure and temperature, ZnO exists in hexagonal wurtzite structure with two lattice parameters, a and c, values of 0.3296 nm and 0.52065 nm respectively (Baruah and Dutta 2009). The hexagonal wurtzite structure of ZnO belongs to the P63mc space group and exhibits a non-centrosymmetric structure, which causes ZnO to be piezoelectric and pyroelectric (Lee et al. 2016).

The wider bandgap energy (3.2–3.7 eV) of ZnO restricts its absorption in the visible region and enhances recombination of charge carriers resulting in low PD efficiency. ZnO photo-corrodes in acidic aqueous suspensions under UV irradiation and suffers dissolution to form $Zn(OH)_2$ on its surface. Photo-corrosion suppresses the dye removal efficiency of ZnO. However, the optical, structural, and magnetic

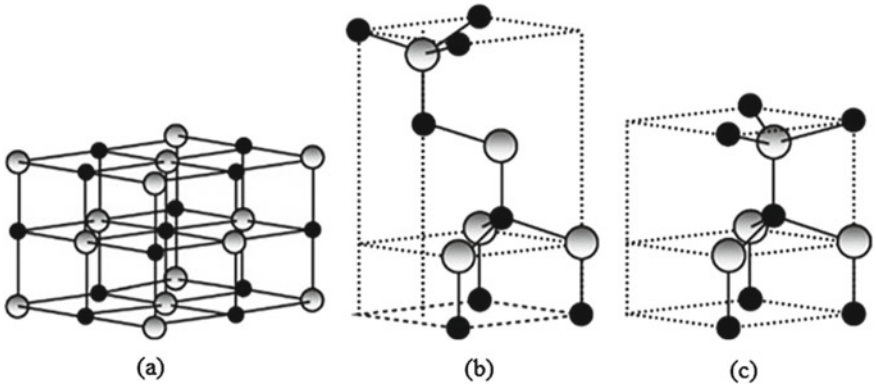

Fig. 2.7 **a** Rocksalt (cubic), **b** zinc blende (cubic) and **c** wurtzite (hexagonal) structures model of ZnO (Lee et al. 2016)

properties of ZnO can be improved and altered by surface modification of the catalysts. The greatest advantage of ZnO is that it can absorb a large portion of the solar spectrum in comparison to TiO_2 (Lee et al. 2016).

2.7.2.1 ZnO Doped Photocatalyst

For improvement of the photocatalytic activity of ZnO, it is modified with the metals that can transfer the photo-response of ZnO in the visible region to maximize photocatalytic efficiency. To counter the recombination of electrons and holes, metal doping is considered as an effective process as it improves the lifetime of charge carriers by enhancing charge separation.

Dopants may also trap the electrons and thus reduce the chances of $e^- - h^+$ recombination and eventually enhancing the PD. The photoactivity of metal-doped semiconductor mostly depends on the concentration and ion nature of the dopant, operating conditions and synthesis method. The incorporation of other elements for the preparation of ZnO photocatalyst is an important challenge. The dopants may be metal or non-metal. The doped ZnO catalyst surpasses its photocatalytic degradation performances. The cationic or metal dopants of ZnO oxide include Li, Na, Ag, W, Cd, Mn, Ni, Pd, Co, Cu. The dopant site of ZnO semiconductors is either a Zn-site or an O-site. Also, it is noticed that the synthesis or substitution of doped catalysts is dependent on the nature of dopants. For example, group-I elements are appropriate for the substitution on Zn-site whilst group-V elements are favourable for substitution on an O-site. Group-I metals like Li^+ have a radius close to Zn^{2+} which favours its incorporation into the ZnO lattice. Transition metals such as Cu^{2+}, Ni^{2+}, Co^{2+}, and Mn^{2+} which are isomorphic to zinc ions are used for the synthesis of doped catalysts. Kumar et al. explained that even 1.0 mol% Fe doped ZnO show better photocatalytic activity towards MB dye degradation (Kumar et al. 2014). Rare earth metals are another important dopant for enhancing photocatalytic degradation. ZnO can also be doped with Er, Hf, where Er-doped ZnO can be prepared through a simple chemical solution route in the absence of surfactant whilst Hf-doped ZnO is prepared by a simple sol–gel method. The Er-doped ZnO showed a better performance in phenol degradation than undoped ZnO which was reported through photoluminescence results (Lam et al. 2012; Din et al. 2021).

Also, non-metal ion doping can improve the photocatalytic degradation performance of ZnO in the visible region compared to pure ZnO. Non-metals such as C, N, F, and S are used as dopants for ZnO. Amongst these non-metals, carbon has a potential advantage due to introducing a new energy level near the ZnO VB edge. As a result, the bandgap energy is reduced and VB is moved to higher energy compared to undoped ZnO and therefore, charge transfer efficiency is increased which enhances the PD (Ullah and Dutta 2008). For N-doped ZnO, incorporation of N occurs into the O site rather than Zn-sites. This modifies the bandgap energy of the catalyst and shifts the absorption efficiency towards visible regions leading to greater PD efficiency (Rajbongshi et al. 2014).

2.7.2.2 Principle of ZnO Photocatalysis and Mechanistic Pathways

Upon irradiation of ZnO in the Ultraviolet (UV) light, the particles absorb photons with energies equal or greater than its bandgap energy. Because of this excitation, the photoinduced electron is promoted from the VB to the CB, forming a positive hole ($h_{VB}{}^{+}$) and electron ($e_{CB}{}^{-}$) on the surface of the ZnO particle (Eq. 2.29). The wavelength for UV light energy typically corresponds to $\lambda < 387$ nm. The bandgap energy depends not only on the crystal structure of the semiconductor but also on its morphology, defects, etc. The reactions of the photocatalytic process are as follows:

$$\mathrm{ZnO} + h\nu(\mathrm{UV}) \rightarrow \mathrm{ZnO}\left(e_{CB}^{-} + h_{VB}^{+}\right) \tag{2.29}$$

$$\mathrm{ZnO}\left(e_{CB}^{-} + h_{VB}^{+}\right) \rightarrow \mathrm{ZnO} + \Delta \tag{2.30}$$

$$\mathrm{ZnO}\left(h_{VB}^{+}\right) + \mathrm{H_2O} \rightarrow \mathrm{ZnO} + \mathrm{H^{+}} + \mathrm{OH^{\bullet}} \tag{2.31}$$

$$\mathrm{ZnO}\left(h_{VB}^{+}\right) + \mathrm{OH^{-}} \rightarrow \mathrm{ZnO} + \mathrm{OH^{\bullet}} \tag{2.32}$$

$$\mathrm{ZnO}\left(e_{CB}^{-}\right) + \mathrm{O_2} \rightarrow \mathrm{ZnO} + \mathrm{O_2^{\bullet -}} \tag{2.33}$$

$$\mathrm{O_2^{\bullet -}} + \mathrm{H^{+}} \rightarrow \mathrm{HO_2^{\bullet}} \tag{2.34}$$

$$\mathrm{HO_2^{\bullet}} + \mathrm{HO_2^{\bullet}} \rightarrow \mathrm{H_2O_2} + \mathrm{O_2} \tag{2.35}$$

$$\mathrm{ZnO}\left(e_{CB}^{-}\right) + \mathrm{H_2O_2} \rightarrow \mathrm{OH^{\bullet}} + \mathrm{OH^{-}} \tag{2.36}$$

$$\mathrm{H_2O_2} + \mathrm{O_2^{\bullet -}} \rightarrow \mathrm{OH^{\bullet}} + \mathrm{OH^{-}} + \mathrm{O_2} \tag{2.37}$$

$$\text{Organic pollutant} + \mathrm{OH^{\bullet}} \rightarrow \text{Degradation products} \tag{2.38}$$

$$\text{Organic pollutant} + \mathrm{ZnO}\left(h_{VB}^{+}\right) \rightarrow \text{Oxidation products} \tag{2.39}$$

$$\text{Organic pollutant} + \mathrm{ZnO}\left(e_{CB}^{-}\right) \rightarrow \text{Reduction products} \tag{2.40}$$

The recombination of photo-generated holes ($h_{VB}{}^{+}$) in the VBand photo-excited electrons ($e_{CB}{}^{-}$) in the CB dissipate as heat (Eq. 2.30). The holes ($h_{VB}{}^{+}$) are then scavenged by oxidizing species {for example, H_2O, OH^{-}, organic compounds, Eqs. (2.32), (2.33) and (2.39)}, and electrons ($e_{CB}{}^{-}$) by reducing species {for example, O_2, Eq. (2.33)} in the solution. The reaction of $h_{VB}{}^{+}$ with OH^{-} (Eq. 2.32)

may lead to the generation of $OH^{\bullet}$ whilst superoxide radical anions ($O_2^{\bullet -}$) are obtained on the reaction of e_{CB}^- with oxygen (Eq. 2.33). The $O_2^{\bullet -}$ then forms hydroperoxyl radicals ($HO_2^{\bullet}$) and subsequently $H_2O_2$by reacting with a surface charge of ZnO (Eqs. 2.34 and 2.35). These radicals are active oxidizing species for the photocatalytic oxidation reaction, which can degrade a variety of organic compounds (toxic and non-toxic) and biological agents (Ullah and Dutta 2008; Lam et al. 2012).

2.7.3 Other Photocatalysts

In the last few decades, various photocatalysts have been reported that are categorized into metal-oxides, metal-sulfides, metal-nitrides, and metal-free compounds like polymers or graphenes. A large variety of entirely novel photoactive semiconductors have been introduced recently as possible substitutes for TiO_2 and ZnO. Amongst these, mixed oxides of transition metal (Nb, V, or Ta) with main group elements such as Ga, In, Sb or Bi have been frequently used to obtain materials with photoactivity in the visible range. In addition, some solids with high surface area, such as cation interchanged zeolites, have been also assessed as photocatalysts, even though they don't have any semiconductor properties. But the photocatalytic activity of other metal oxides is considered to be relatively weak in comparison to the TiO_2. Nevertheless. metal oxides like Cu_2O, WO_3 have found application in the photodegradation of polyethylene plastic and organic dyes respectively (Bedja et al. 2002). Further, Nb_2O_5 strongly increases TiO_2 activity towards the degradation of dichloro-benzene and In_2O_3 helps in the photodegradation of ethane (Ishchenko et al. 2016; Hernández-Alonso 2009).

Semiconductors such as ZnS, CdS, $SrTiO_3$, MoS_2, GaP are also frequently used as photocatalysts. For example, GaP and CdS were used for the synthesis of NH_3 from water and nitrogen with a better yield compared to TiO_2 or ZnO. This process is favourable when the conduction band energy of the semiconductor becomes more negative. This can be explained by the greater affinity of photoexcited electrons to reduce nitrogen in a more negative conduction band. Larger yields were reached when Pt black was incorporated into the catalyst (Hernández-Alonso et al. 2009). CdS can also absorb visible light owing to its short bandgap (2.42 eV) which makes it a potential catalyst for photocatalysis and solar cells. In (2016), Samadi-Maybodi and Sadeghi-Maleki developed a method for *in-situ* generation of stable CdS quantum dots (CdS-QD) using $Na_2S_2O_3$ as a precursor and thioglycolic acid as a catalyst as well as capping agent. Good photocatalytic activity and recycling stability were shown by CdS-QD under visible light irradiation compared to the bulk CdS for degradation of alizarin, mordant red (MR), acid violet (AV), and thymol blue (TB) (Samadi-Maybodi and Sadeghi-Maleki 2016).

2.8 Application of Heterogeneous Photocatalysis

Heterogeneous photocatalysis has grown rapidly in recent years and experienced various developments especially concerning energy and the environment. Solar water splitting, purification of air and water containing low concentrations of pollutants are the two most important applications of heterogeneous photocatalysis. It has been successfully utilized by different developing countries to eliminate pathogens and algal blooms in freshwater supplies. Heterogeneous photocatalysis is a very cheap technique compared to reverse osmosis and ultra or nanofiltration. Humic substances which help in bacterial growth can be treated by TiO_2 assisted photosensitized disinfection. The multidisciplinary nature of the process is extended semiconductor physics, surface sciences, materials science, photo and physical chemistry, and chemical engineering (Fujishima et al. 2000; Ibhadon and Fitzpatrick 2013). The various applications of photocatalysis are shown in Fig. 2.8.

Fig. 2.8 Various applications of heterogeneous photocatalysis

2.8.1 Self-Cleaning

- Heterogeneous photocatalysis has found application in the self-cleaning process of materials for residential and office buildings in exterior tiles, kitchen and bathroom components, interior furnishings, plastic surfaces, aluminum siding, building stone, curtains, and paper window blinds.
- Photocatalysis can also be utilized in indoor and outdoor lamps like translucent paper for indoor lamp covers, coatings for fluorescent lamps, and a cover glass of highway tunnel lamps.
- For other road materials such as tunnel wall, soundproofed wall, traffic signs, and reflectors as well as for tent material, for hospital garments, uniforms as well as spray coatings for cars.

2.8.2 Air Cleaning

- The methods can be used in indoor and outdoor air cleaning. Photocatalyst-equipped air conditioners for rooms and factories are some indoor applications.

2.8.3 Application for Water and Wastewater Treatment

Due to the growth in the global population, the supply of clean water has now been diminished which heightened the environmental concerns. Thus, the employment of effective sustainable water treatment technology has drawn much attention considering the high requirement of clean water. For water purification and treatment, advanced oxidation processes (AOPs) have shown tremendous potential in the elimination of naturally occurring toxins, pesticides, and other deleterious contaminants. UV light-assisted photocatalytic systems are useful for the treatment of water containing trace amounts of pollutants (such as estrogens) and also for industrial wastewater treatment which contains a high load of organic pollutants. Photocatalysis with nanocatalysts and membrane filtration are some promising methods for disinfection with high water cleaning efficiency (Ibhadon and Fitzpatrick 2013).

Different photocatalytic materials can be used for the decomposition of humic substances present in both highly saline and seawater. The rate of decomposition of humic substances was fast in pure water as compared to seawater media and during the process of decomposition, no toxic by-products were detected. Another study found that the decomposition of seawater-soluble crude-oil fractions was achieved using TiO_2 nanoparticles under artificial light irradiation. Photocatalysis techniques are also used to kill bacteria and viruses present in water bodies. Algal blooms found in freshwater supplies are also degraded on an immobilized TiO_2 catalyst. Degradation of the green algae having thick cell walls by photo disinfection sensitized by TiO_2 has

been applied greatly to treat water especially in remote and disaster areas of many developed and developing countries (Fukushima et al. 2000; Ahmed and Haider 2018).

2.8.4 Removal of Trace Metals

Heavy metals such as Hg, Cr, Pb, Ni, Cu, etc. are highly hazardous to human health. Removal of these toxic heavy materials from freshwater can be obtained by the application of heterogeneous photocatalysis. Again, photoreduction by photocatalysts has been applied in the extraction of expensive metals, such as Au, Pt, and Ag from industrial effluents (Uyguner and Bekbolet 2008).

2.8.5 Removal of Inorganic Compounds

Several inorganic compounds are also sensitive like organic compounds to photochemical transformation on the catalyst surface. Inorganic species such as BrO_3^-, ClO_4^-, N_3^-, NO, halide ions, Pd- and Rh- species, sulfur species, metal salts like $AgNO_3$, HgCl, organometallic compound (e.g., CH_3HgCl) can be decomposed and removed using heterogeneous photocatalysis (Uyguner and Bekbolet 2008).

2.8.6 Applications in Photodynamic Therapy

Photocatalysis has significant application for the treatment of different cancer cells such as colon or kidney cancer (tumour therapy). This technique has also responded well to the treatment of tumours in rats. Generally, TiO_2 is introduced in cancer sites and photosensitized using an optic fibre cable to introduce the illumination. Thus, reactive oxygen species are generated during activation of photosensitizer on illumination that destroys the tumour cells (Al-Mamun et al. 2019).

Heterogeneous photocatalysis has found applications in hospitals garments worn during operations that have 'doses' of TiO_2 added to the fabric. TiO_2 fabrics control infections in hospital garments, methicillin-resistant *Staphylococcus* (MRSA) as well as antimicrobial photodynamic therapy (APDT) is used to decolonize MRSA from patients (Fujishima et al. 2000).

2.9 Conclusion and Outlook

In this chapter, we attempt to assess and summarize the latest work on heterogeneous photocatalytic degradation of organic effluents using both pure and doped catalysts. The chapter comprises the type of dyes their impact on the environment; advancements to enhance photocatalytic efficiency; the effects of key operational parameters on the photocatalytic performance are detailed. A brief synopsis of the application of heterogeneous photocatalysis in various fields is also given. The principle of photocatalytic activity of metal oxides in particular ZnO and TiO_2 is discussed in detail. The non-toxic ZnO and TiO_2 semiconductors are used to convert effluents to lesser toxic forms. Apart from metal oxides, other low bandgap semiconductors and their modified form should be explored extensively. As per reported literature, the surface morphology of photocatalyst has a great impact on catalytic efficiency. Thus, for designing of novel catalytic system, the optimization of the key parameters is very important for a smooth operation. In the real world, pollutants present in wastewater are a mixture of various contaminants. Thus, future research must be focused on the development of techniques for multi-components rather than a single pollutant. For smooth industrial-scale applications, the economic practicability of a heterogeneous catalyst is another aspect that needs alarming attention.

References

Abdullah FH, Rauf MA, Ashraf SS (2007) Kinetics and optimization of photolytic decolouration of carmine by UV/H2O2. Dyes Pigm 75:194–198

Abid MF, Zablouk MA, Abid-Alameer AM (2012) Experimental study of dye removal from industrial wastewater by membrane technologies of reverse osmosis and nanofiltration. J Environ Health Sci Engineer 9:17

Ahmed SN, Haider W (2018) Heterogeneous photocatalysis and its potential applications in water and wastewater treatment: a review. Nanotechnology 29:342001

Ahmed S, Rasul MG, Brown R, Hashib MA (2011) Influence of parameters on the heterogeneous photocatalytic degradation of pesticides and phenolic contaminants in wastewater: a short review. J Environ Manage 92:311–330

Ajaz M, Rehman A, Khan Z, Nisar MA, Hussain S (2019) Degradation of azo dyes by Alcaligenes aquatilis 3c and its potential use in the wastewater treatment. AMB Expr 9:64

Akpan UG, Hameed BH (2009) Parameters affecting the photocatalytic degradation of dyes using TiO_2-based photocatalysts: a review. J Hazard Mater 170:520–529

Alahiane S, Sennaoui A, Sakr F, Qourzal S, Dinne M, Assabbane A (2017) A study of the photocatalytic degradation of the textile dye reactive yellow 17 in aqueous solution by TiO_2-coated non-woven fibres in a batch photoreactor. J Mater Environ Sci 8:3556–3563

Al-Mamun MR, Kader S, Islam MS, Khan MZH (2019) Photocatalytic activity improvement and application of UV-TiO_2 photocatalysis in textile wastewater treatment: a review. J Environ Chem Eng 7:103248

Alnuaimi MM, Rauf MA, Ashraf SS (2007) Comparative decolouration study of neutral red by different oxidative processes. Dyes Pigm 72:367–371

Andronic L, Duta A (2007) TiO_2 thin films for dyes photodegradation. Thin Solid Films 515:6294–6297

Anwer H, Mahmood A, Lee J, Kim K-H, Park J-W, Yip ACK (2019) Photocatalysts for degradation of dyes in industrial effluents: opportunities and challenges. Nano Res 12:955–972

Atarod M, Nasrollahzadeh M, Mohammad Sajadi S (2016) Euphorbia heterophylla leaf extract mediated green synthesis of Ag/TiO_2 nanocomposite and investigation of its excellent catalytic activity for reduction of variety of dyes in water. J Colloid Interface Sci 462:272–279

Babu SG, Karthik P, John MC, Lakhera SK, Ashokkumar M, Khim J, Neppolian B (2019) Synergistic effect of sono-photocatalytic process for the degradation of organic pollutants using CuO-TiO_2/rGO. Ultrason Sonochem 50:218–223

Bandara WRLN, de Silva RM, de Silva KMN, Dahanayake D, Gunasekara S, Thanabalasingam K (2017) Is nano ZrO_2 a better photocatalyst than nano TiO_2 for degradation of plastics? RSC Adv 7:46155–46163

Baran W, Makowski A, Wardas W (2008) The effect of UV radiation absorption of cationic and anionic dye solutions on their photocatalytic degradation in the presence TiO_2. Dyes Pigm 76:226–230

Baruah S, Dutta J (2009) Hydrothermal growth of ZnO nanostructures. Sci Technol Adv Mater 10:013001

Behnajady MA, Modirshahla N, Shokri M (2004) Photodestruction of Acid Orange 7 (AO7) in aqueous solutions by UV/H_2O_2: influence of operational parameters. Chemosphere 55:129–134

Bedja I, Hotchandani S, Kamat PV (2002) Photoelectrochemistry of quantized WO_3 colloids: electron storage, electrochromic, and photoelectrochromic effects. J Phys Chem 97:11064–11070

Belpaire C, Reyns T, Geeraerts C, Van Loco J (2015) Toxic textile dyes accumulate in wild European eel Anguilla anguilla. Chemosphere 138:784–791

Benatti CT, Tavares CRG, Guedes TA (2006) Optimization of Fenton's oxidation of chemical laboratory wastewaters using the response surface methodology. J Environ Manage 80:66–74

Ben Fradj A, Boubakri A, Amor H, Hamouda S (2019) Removal of azoic dyes from aqueous solutions by chitosan enhanced ultrafiltration. Results Chem 2:100017

Benkhaya S, M' rabet S, El Harfi A, (2020) A review on classifications, recent synthesis and applications of textile dyes. Inorg Chem Commun 115:107891

Blanco-Galvez J, Fernández-Ibáñez P, Malato-Rodríguez S (2007) Solar photocatalytic detoxification and disinfection of water: recent overview. J Sol Energy Eng 129:4–15

Chandanshive VV, Kadam SK, Khandare RV, Kurade MB, Jeon B-H, Jadhav JP, Govindwar SP (2018) In situ phytoremediation of dyes from textile wastewater using garden ornamental plants, effect on soil quality and plant growth. Chemosphere 210:968–976

Chen D, Cheng Y, Zhou N, Chen P, Wang Y, Li K, Huo S, Cheng P, Peng P, Zhang R, Wang L, Liu H, Liu Y, Ruan R (2020) Photocatalytic degradation of organic pollutants using TiO2-based photocatalysts: a review. J Clean Prod 268:121725

Chequer FMD, Oliveira GAR de, Ferraz ERA, Cardoso JC, Zanoni MVB, Oliveira DP de (2013) Textile dyes: dyeing process and environmental impact. IntechOpen, pp 151–176

Che Ramli ZA, Asim N, Isahak WNRW, Emdadi Z, Ahmad-Ludin N, Yarmo MA, Sopian K (2014) Photocatalytic degradation of methylene blue under UV light irradiation on prepared carbonaceous TiO_2. Sci World J 2014:1–8

Chen X, Wu Z, Liu D, Gao Z (2017) Preparation of ZnO photocatalyst for the efficient and rapid photocatalytic degradation of azo dyes. Nanoscale Res Lett 12:143

Crini G, Lichtfouse E (2019) Advantages and disadvantages of techniques used for wastewater treatment. Environ Chem Lett 17:145–155

Dahiya A, Patel BK (2021) Photocatalytic degradation of organic dyes using heterogeneous catalysts. In: Photocatalytic degradation of dyes. Elsevier, pp 43–90

Daneshvar N, Salari D, Khataee AR (2003) Photocatalytic degradation of azo dye acid red 14 in water: investigation of the effect of operational parameters. J Photochem Photobiol A Chem 157:111–116

Din MI, Khalid R, Hussain Z (2021) Recent research on development and modification of nontoxic semiconductor for environmental application. Sep Purif Rev 50:244–261

Dionysiou DD, Khodadoust AP, Kern AM, Suidan MT, Baudin I, Laîné J-M (2000) Continuous-mode photocatalytic degradation of chlorinated phenols and pesticides in water using a bench-scale TiO_2 rotating disk reactor. Appl Catal B24:139–155

Drumond CFM, de Oliveira GAR, Ferraz ERA, Carvalho J, Zanoni MVB, de Oliveir DP (2013) Textile dyes: dyeing process and environmental impact. In: Gunay M (ed) Eco-Friendly Textile Dyeing and Finishing. InTech. 10.5772/53659

Es-sahbany H, Berradi M, Nkhili S, Bassir D, Belfaquir M, Youbi MSE (2018) Valorization of Moroccan clay: application to the adsorption of cobalt ions contained in wastewater synthesized. Mor J Chem 6:173–179

Fenoll J, Martínez-Menchón M, Navarro G, Vela N, Navarro S (2013) Photocatalytic degradation of substituted phenylurea herbicides in aqueous semiconductor suspensions exposed to solar energy. Chemosphere 91:571–578

Ferreira ESB, Hulme AN, McNab H, Quye A (2004) The natural constituents of historical textile dyes. Chem Soc Rev 33:329–336

Franca RDG, Vieira A, Carvalho G, Oehmen A, Pinheiro HM, Barreto Crespo MT, Lourenço ND (2020) Oerskovia paurometabola can efficiently decolourize azo dye Acid Red 14 and remove its recalcitrant metabolite. Ecotoxicol Environ Saf 191:110007

Fujishima A, Honda K (1972) Electrochemical photolysis of water at a semiconductor electrode. Nature 238:37–38

Fujishima A, Rao TN, Tryk DA (2000) Titanium dioxide photocatalysis. J Photochem Photobiol C 1:1–21

Fukushima M, Tatsumi K, Morimoto K (2000) Influence of iron(III) and humic acid on the photodegradation of pentachlorophenol. Environ Toxicol Chem 19:1711–1716

Garg A, Singhania T, Singh A, Sharma S, Rani S, Neogy A, Yadav SR, Sangal VK, Garg N (2019) Photocatalytic degradation of bisphenol-a using N, Co codoped TiO_2catalyst under solar light. Sci Rep 9:765

Gnanaprakasam A, Sivakumar VM, Thirumarimurugan M (2015) Influencing parameters in the photocatalytic degradation of organic effluent via nanometal oxide catalyst: a review. Indian J Mater Sci 2015:1–16

Haibach MC, Kundu S, Brookhart M, Goldman AS (2012) Alkane metathesis by tandem alkane-dehydrogenation–olefin-metathesis catalysis and related chemistry. Acc Chem Res 45:947–958

Hassena H (2016) Photocatalytic degradation of methylene blue by using Al_2O_3/Fe_2O_3nano composite under visible light. Mod Chem Appl 4:176

Haq I, Raj A, Markandeya (2018) Biodegradation of Azure-B dye by Serratia liquefaciens and its validation by phytotoxicity, genotoxicity and cytotoxicity studies. Chemosphere 196:58–68

Hasnat M, Uddin M, Samed A, Alam S, Hossain S (2007) Adsorption and photocatalytic decolourization of a synthetic dye erythrosine on anatase TiO2 and ZnO surfaces. J Hazard Mater 147:471–477

Hernández-Alonso MD, Fresno F, Suárez S, Coronado JM (2009) Development of alternative photocatalysts to TiO2: challenges and opportunities. Energy Environ Sci 2:1231

Holkar CR, Jadhav AJ, Pinjari DV, Mahamuni NM, Pandit AB (2016) A critical review on textile wastewater treatments: possible approaches. J Environ Manage 182:351–366

Hu C, Yu JC, Hao Z, Wong PK (2003) Effects of acidity and inorganic ions on the photocatalytic degradation of different azo dyes. Appl Catal B 46:35–47

Ibhadon AO, Fitzpatrick P (2013) Heterogeneous photocatalysis: recent advances and applications. Catalysts 3:189–218

Ishchenko OM, Rogé V, Lamblin G, Lenoble D (2016) TiO_2- and ZnO-based materials for photocatalysis: material properties, device architecture and emerging concepts. In: Cao W (ed) Semiconductor photocatalysis—materials, mechanisms and applications. InTech

Ito T, Adachi Y, Yamanashi Y, Shimada Y (2016) Long-term natural remediation process in textile dye-polluted river sediment driven by bacterial community changes. Water Res 100:458–465

Jadhav SB, Yedurkar SM, Phugare SS, Jadhav JP (2012) Biodegradation studies on acid violet 19, a triphenylmethane dye, by pseudomonas aeruginosa BCH. Clean Soil Air Water 40:551–558

Javaid R, Qazi UY, Kawasaki S-I (2016) Highly efficient decomposition of Remazol Brilliant Blue R using tubular reactor coated with thin layer of PdO. J Environ Manage 180:551–556
Javaid R, Qazi UY, Ikhlaq A, Zahid M, Alazmi A (2021) Subcritical and supercritical water oxidation for dye decomposition. J Environ Manage 290:112605
Khan S, Malik A (2018) Toxicity evaluation of textile effluents and role of native soil bacterium in biodegradation of a textile dye. Environ Sci Pollut Res Int 25:4446–4458
Khataee AR, Kasiri MB (2010) Photocatalytic degradation of organic dyes in the presence of nanostructured titanium dioxide: influence of the chemical structure of dyes. J Mol Catal A Chem 328:8–26
Kiran Avasarala B, Tirukkovalluri SR (2016) Magnesium doped titania for photocatalytic degradation of dyes in visible light. J Environ Anal Toxicol 6:2
Kong G, Pang J, Tang Y, Fan L, Sun H, Wang R, Feng S, Feng Y, Fan W, Kang W, Guo H, Kang Z, Sun D (2019) Efficient dye nanofiltration of a graphene oxide membrane via combination with a covalent organic framework by hot pressing. J Mater Chem A 7:24301–24310
Kuang S, Yang L, Luo S, Cai Q (2009) Fabrication, characterization and photoelectrochemical properties of Fe_2O_3 modified TiO_2 nanotube arrays. Appl Surf Sci 255:7385–7388
Kumar K, Chitkara M, Sandhu IS, Mehta D, Kumar S (2014) Photocatalytic, optical and magnetic properties of Fe-doped ZnO nanoparticles prepared by chemical route. J Alloys Compd 588:681–689
Kushniarou A, Garrido I, Fenoll J, Vela N, Flores P, Navarro G, Hellín P, Navarro S (2019) Solar photocatalytic reclamation of agro-waste water polluted with twelve pesticides for agricultural reuse. Chemosphere 214:839–845
Lachheb H, Puzenat E, Houas A, Ksibi M, Elaloui E, Guillard C, Herrmann J-M (2002) Photocatalytic degradation of various types of dyes (Alizarin S, Crocein Orange G, Methyl Red, Congo Red, Methylene Blue) in water by UV-irradiated titania. Appl Catal B 39:75–90
Lai C, Wang M-M, Zeng G-M, Liu Y-G, Huang D-L, Zhang C, Wang R-Z, Xu P, Cheng M, Huang C, Wu H-P, Qin L (2016) Synthesis of surface molecular imprinted TiO_2/graphene photocatalyst and its highly efficient photocatalytic degradation of target pollutant under visible light irradiation. Appl Surf Sci 390:368–376
Lakshmi Prasanna V, Rajagopalan V (2016) A new synergetic nanocomposite for dye degradation in dark and light. Sci Rep 6:38606
Lam S-M, Sin J-C, Abdullah AZ, Mohamed AR (2012) Degradation of wastewaters containing organic dyes photocatalysed by zinc oxide: a review. Desalination Water Treat 41:131–169
Lee KM, Lai CW, Ngai KS, Juan JC (2016) Recent developments of zinc oxide based photocatalyst in water treatment technology: a review. Water Res 88:428–448
Lewis DM (2011) The chemistry of reactive dyes and their application processes. In: Handbook of textile and industrial dyeing. Elsevier, pp 303–364
Li FB, Li XZ (2002) The enhancement of photodegradation efficiency using Pt–TiO_2 catalyst. Chemosphere 48:1103–1111
Lin X, Liu Z, Guo X, Liu C, Zhai H, Wang Q, Chang L (2014) Controllable synthesis and photocatalytic activity of spherical, flower-like and nanofibrous bismuth tungstates. Mater Sci Eng B188:35–42
Liu F, Leung YH, Djurišić AB, Ng AMC, Chan WK (2013) Native defects in ZnO: effect on dye adsorption and photocatalytic degradation. J Phys Chem C 117:12218–12228
Li Y, He J, Zhang K, Hong P, Wang C, Kong L, Liu J (2020) Oxidative degradation of sulfamethoxazole antibiotic catalyzed by porous magnetic manganese ferrite nanoparticles: mechanism and by-products identification. J Mater Sci 55:13767–13784
López-Ramón MV, Rivera-Utrilla J, Sánchez-Polo M, Polo AMS, Mota AJ, Orellana-García F, Álvarez MA (2019) Photocatalytic oxidation of diuron using nickel organic xerogel under simulated solar irradiation. Sci Total Environ 650:1207–1215
Luttrell T, Halpegamage S, Tao J, Kramer A, Sutter E, Batzill M (2015) Why is anatase a better photocatalyst than rutile?—model studies on epitaxial TiO_2 films. Sci Rep 4:4043

Lü W, Chen J, Wu Y, Duan L, Yang Y, Ge X (2014) Graphene-enhanced visible-light photocatalysis of large-sized CdS particles for wastewater treatment. Nanoscale Res Lett 9:148

Moura DC de, Quiroz MA, Silva DR da, Salazar R, Martínez-Huitle CA (2016) Electrochemical degradation of Acid Blue 113 dye using TiO_2-nanotubes decorated with PbO_2 as anode. Environ Nanotechnol Monit Manag 13–20

Mozia S, Tomaszewska M, Morawski AW (2005) Photocatalytic degradation of azo-dye acid red 18. Desalination 185:449–456

Muruganandham M, Swaminathan M (2006) TiO_2–UV photocatalytic oxidation of reactive yellow 14: effect of operational parameters. J Hazard Mater 135:78–86

Neppolian B, Choi HC, Sakthivel S, Arabindoo B, Murugesan V (2002) Solar/UV-induced photocatalytic degradation of three commercial textile dyes. J Hazard Mater 89:303–317

Olama N, Dehghani M, Malakootian M (2018) The removal of amoxicillin from aquatic solutions using the TiO_2/UV-C nanophotocatalytic method doped with trivalent iron. Appl Water Sci 8:97

Ollis DF, Pelizzetti E, Serpone N (1991) Destruction of water contaminants. Environ Sci Technol 25:1522–1529

Pan L, Zou J-J, Zhang X, Wang L (2010) Photoisomerization of norbornadiene to quadricyclane using transition metal doped TiO_2. Ind Eng Chem Res 49:8526–8531

Pelaez M, Nolan NT, Pillai SC, Seery MK, Falaras P, Kontos AG, Dunlop PSM, Hamilton JWJ, Byrne JA, O'Shea K, Entezari MH, Dionysiou DD (2012) A review on the visible light active titanium dioxide photocatalysts for environmental applications. Appl Catal B 125:331–349

Pingmuang K, Chen J, Kangwansupamonkon W, Wallace GG, Phanichphant S, Nattestad A (2017) Composite photocatalysts containing $BiVO_4$ for degradation of cationic dyes. Sci Rep 7:8929

Poulopoulos SG, Philippopoulos CJ (2004) Photo-assistedo of chlorophenols in aqueous Solutions using hydrogen peroxide and titanium dioxide. J Environ Sci Health A 39:1385–1397

Prihod'ko RV, Soboleva NM (2013) Photocatalysis: oxidative processes in water treatment. J Chem e168701

Qamar M, Saquib M, Muneer M (2004) Photocatalytic degradation of two selected dye derivatives, chromotrope 2B and amido black 10B, in aqueous suspensions of titanium dioxide. Dyes Pigm 65:1–9

Rahmat M, Rehman A, Rahmat S, Bhatti HN, Iqbal M, Khan WS, Bajwa SZ, Rahmat R, Nazir A (2019) Highly efficient removal of crystal violet dye from water by MnO_2 based nanofibrous mesh/photocatalytic process. J Mater Res Technol 8:5149–5159

Rajabi HR, Khani O, Shamsipur M, Vatanpour V (2013) High-performance pure and Fe^{3+}-ion doped ZnS quantum dots as green nanophotocatalysts for the removal of malachite green under UV-light irradiation. J Hazard Mater 250–251:370–378

Rajbongshi BM, Ramchiary A, Samdarshi S (2014) Influence of N-doping on photocatalytic activity of ZnO nanoparticles under visible light irradiation. Mater Lett 134:111–114

Rauf MA, Ashraf SS (2009) Fundamental principles and application of heterogeneous photocatalytic degradation of dyes in solution. Chem Eng Technol 151:10–18

Ray MB (2000) Photodegradation of the volatile organic compounds in the gas phase: a review. Chem Eng Process 8:405–439

Reddy ChV, Babu B, Reddy IN, Shim J (2018) Synthesis and characterization of pure tetragonal ZrO_2 nanoparticles with enhanced photocatalytic activity. Ceram Int 44:6940–6948

Rehman A, Usman M, Bokhari TH, Haq A, Saeed M, Rahman HMA, Siddiq M, Rasheed A, Nisa M (2020) The application of cationic-nonionic mixed micellar media for enhanced solubilization of Direct Brown 2 dye. Jmol Liq 301:112408

Rehman R, Uz-Zaman W, Abbas A, Mitu L (2019) Rapid photocatalytic degradation of methylene blue, tartrazine and brilliant green dyes by high-flux UV irradiation photolysis reactor. BCC 51:337–341

Saeed K, Khan I, Park S-Y (2015) TiO_2/amidoxime-modified polyacrylonitrile nanofibres and its application for the photodegradation of methyl blue in aqueous medium. Desalin Water Treat 54:3146–3151

Sahel K, Perol N, Chermette H, Bordes C, Derriche Z, Guillard C (2007) Photocatalytic decolourization of Remazol Black 5 (RB5) and Procion Red MX-5B—isotherm of adsorption, kinetic of decolourization and mineralization. Appl Catal B 77:100–109

Sahoo C, Gupta AK, Pillai IMS (2012) Photocatalytic degradation of methylene blue dye from aqueous solution using silver ion-doped TiO2 and its application to the degradation of real textile wastewater. J Environ Sci Health Part A 47:1428–1438

Sakthivel S, Neppolian B, Shankar MV, Arabindoo B, Palanichamy M, Murugesan V (2003) Solar photocatalytic degradation of azo dye: comparison of photocatalytic efficiency of ZnO and TiO_2. Sol Energy Mater Sol Cells 77:65–82

Salem IA, El-Ghamry HA, El-Ghobashy MA (2014) Catalytic decolourization of acid blue 29 dye by H_2O_2 and a heterogeneous catalyst. Beni-Seuf Univ J Basic Appl Sci 3:186–192

Samadi-Maybodi A, Sadeghi-Maleki M-R (2016) In-situ synthesis of high stable CdS quantum dots and their application for photocatalytic degradation of dyes. Spectrochimica Acta Part A Spectrochim Acta A Mol Biomol Spectrosc 152:156–164

Serpone N, Emeline AV (2002) Suggested terms and definitions in photocatalysis and radiocatalysis. Int J Photoenergy 4:91–131

Sharma S, Hasan A, Kumar N, Pandey LM (2018) Removal of methylene blue dye from aqueous solution using immobilized Agrobacterium fabrum biomass along with iron oxide nanoparticles as biosorbent. Environ Sci Pollut Res Int 25:21605–21615

Silva PM dos S, Fiaschitello TR, Queiroz RS de, Freeman HS, Costa SA da, Leo P, Montemor AF, Costa SM da (2020) Natural dye from Croton urucurana Baill. bark: extraction, physicochemical characterization, textile dyeing and colour fastness properties. Dyes Pigm 173:107953

Solís M, Solís A, Pérez HI, Manjarrez N, Flores M (2012) Microbial decolouration of azo dyes: a review. Process Biochem 47:1723–1748

Sripiboon S, Suwannahong K (2018) Colour removal by ozonation process in biological wastewater treatment from the breweries. IOP Conf Ser Earth Environ Sci 167:012010

Štengl V, Bakardjieva S, Murafa N (2009) Preparation and photocatalytic activity of rare earth doped TiO_2 nanoparticles. Mater Chem Phys 114:217–226

Stylidi M (2003) Pathways of solar light-induced photocatalytic degradation of azo dyes in aqueous TiO_2 suspensions. Appl Catal B 40:271–286

Su B, Wang K, Bai J, Mu H, Tong Y, Min S, She S, Lei Z (2007) Photocatalytic degradation of methylene blue on Fe^{3+}-doped TiO_2 nanoparticles under visible light irradiation. Front Chem China 2:364–368

Tanaka K, Padermpole K, Hisanaga T (2000) Photocatalytic degradation of commercial azo dyes. Water Res 34:327–333

Tayade RJ, Natarajan TS, Bajaj HC (2009) Photocatalytic degradation of methylene blue dye using ultraviolet light emitting diodes. Ind Eng Chem Res 48:10262–10267

Tkaczyk A, Mitrowska K, Posyniak A (2020) Synthetic organic dyes as contaminants of the aquatic environment and their implications for ecosystems: a review. Sci Total Environ 717:137222

Touati A, Hammedi T, Najjar W, Ksibi Z, Sayadi S (2016) Photocatalytic degradation of textile wastewater in presence of hydrogen peroxide: effect of cerium doping Titania. J Ind Eng Chem J 35:36–44

Ullah R, Dutta J (2008) Photocatalytic degradation of organic dyes with manganese-doped ZnO nanoparticles. J Hazard Mater 156:194–200

Uyguner CS, Bekbolet M (2008) Aqueous photocatalysis, natural organic matter characterization and removal: a case study of the photacatalytic oxidation of fulvic acid. Dangerous pollutants (xenobiotics) in urban water cycle. Springer, Netherlands, Dordrecht, pp 247–256

Vázquez-Ortega F, Lagunes I, Trigos Á (2020) Cosmetic dyes as potential photosensitizers of singlet oxygen generation. Dyes Pigm 176:108248

Vinu R, Akki SU, Madras G (2010) Investigation of dye functional group on the photocatalytic degradation of dyes by nano-TiO2. J Hazard Mater 176:765–773

Wang F, Ma Z, Ban P, Xu X (2017) C, N and S codoped rutile TiO_2 nanorods for enhanced visible-light photocatalytic activity. Mater Lett 195:143–146

Wang N, Li J, Zhu L, Dong Y, Tang H (2008) Highly photocatalytic activity of metallic hydroxide/titanium dioxide nanoparticles prepared via a modified wet precipitation process. J Photochem Photobiol A 198:282–287

Wang Z, Gao M, Li X, Ning J, Zhou Z, Li G (2020) Efficient adsorption of methylene blue from aqueous solution by graphene oxide modified persimmon tannins. Mater Sci Eng C Mater Biol Appl 108:110196

Wu C-H, Chang H-W, Chern J-M (2006) Basic dye decomposition kinetics in a photocatalytic slurry reactor. J Hazard Mater 137:336–343

Yan-fen F, Ying-ping H, De-fu L, Yang H, Wei G, Johnson D (2006) Photocatalytic degradation of the dye sulforhodamine-B: a comparative study of different light sources. Res J Environ Sci 19:97–102

Yoon J, Lee Y, Kim S (2001) Investigation of the reaction pathway of OH radicals produced by Fenton oxidation in the conditions of wastewater treatment. Water Sci Technol 44:15–21

Yuan H, Chen L, Cao Z, Hong F (2020) Enhanced decolourization efficiency of textile dye Reactive Blue 19 in a horizontal rotating reactor using strips of BNC-immobilized laccase: Optimization of conditions and comparison of decolourization efficiency. Biochem Eng J 156:107501

Zada N, Khan I, Saeed K (2017) Synthesis of multiwalled carbon nanotubes supported manganese and cobalt zinc oxides nanoparticles for the photodegradation of malachite green. Sep Sci Technol 52:1477–1485

Zahrim AY, Hilal N (2013) Treatment of highly concentrated dye solution by coagulation/flocculation–sand filtration and nanofiltration. Water Resour Ind 3:23–34

Zangeneh H, Zinatizadeh AAL, Habibi M, Akia M, Hasnain Isa M (2015) Photocatalytic oxidation of organic dyes and pollutants in wastewater using different modified titanium dioxides: a comparative review. J Ind Eng Chem 26:1–36

Zazo JA, Pliego G, Blasco S, Casas JA, Rodriguez JJ (2011) Intensification of the Fenton process by increasing the temperature. Ind Eng Chem Res 50:866–870

Zhang G, Zhang S (2020) Quantitative structure-activity relationship in the photodegradation of azo dyes. J Environ Sci (china) 90:41–50

Zhang L, Jaroniec M (2017) Toward designing semiconductor-semiconductor heterojunctions for photocatalytic applications. Appl Surf Sci 430:2–17

Zhang T, Oyama T, Horikoshi S, Hidaka H, Zhao J, Serpone N (2002) Photocatalyzed N-demethylation and degradation of methylene Blue in titania dispersions exposed to concentrated sunlight. Sol Energy Mater Sol Cells 73:287–303

Zhang X, Wu Y, Xiao G, Tang Z, Wang M, Liu F, Zhu X (2017) Simultaneous photocatalytic and microbial degradation of dye-containing wastewater by a novel g-C3N4-P25/photosynthetic bacteria composite. PLoS ONE 12:e0172747

Zhao J, Chen C, Ma W (2005) Photocatalytic degradation of organic pollutants under visible light irradiation. Top Catal 35:269–278

Zheng Y, Cao L, Xing G, Bai Z, Huang J, Zhang Z (2019) Microscale flower-like magnesium oxide for highly efficient photocatalytic degradation of organic dyes in aqueous solution. RSC Adv 9:7338–7348